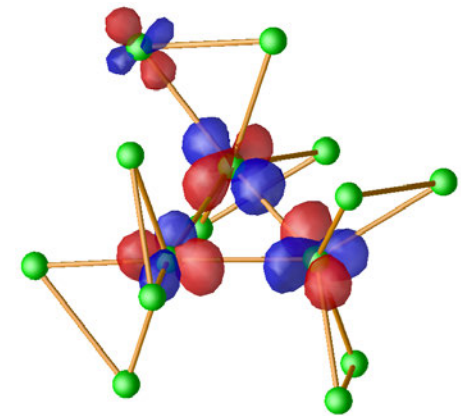
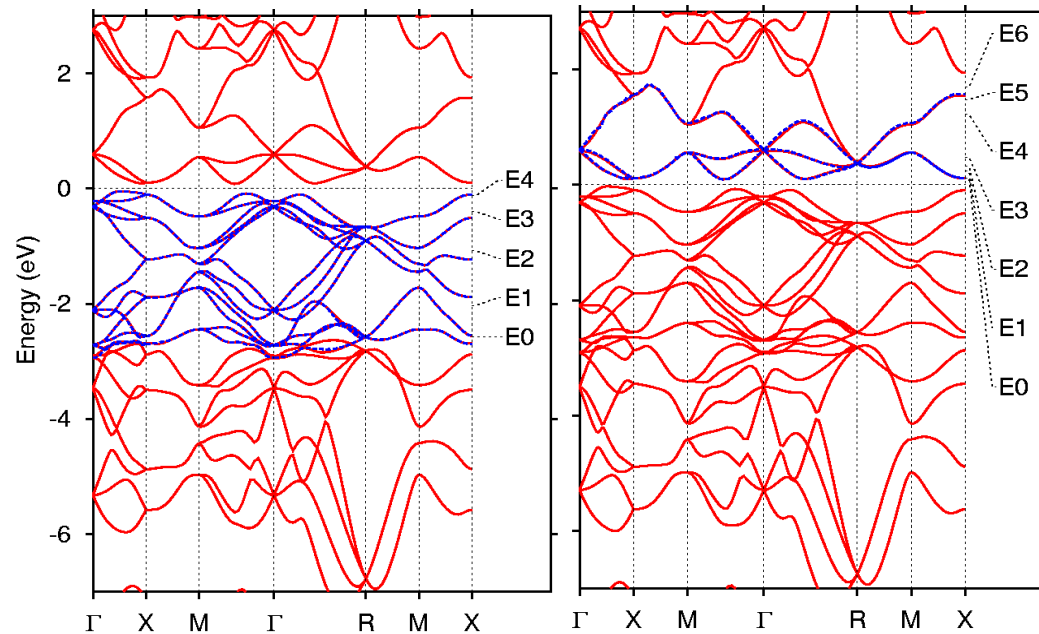
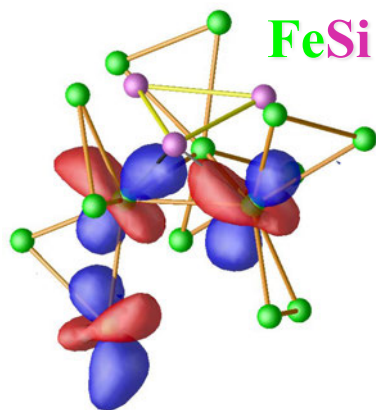


NMTOs and their Wannier functions

O. K. Andersen

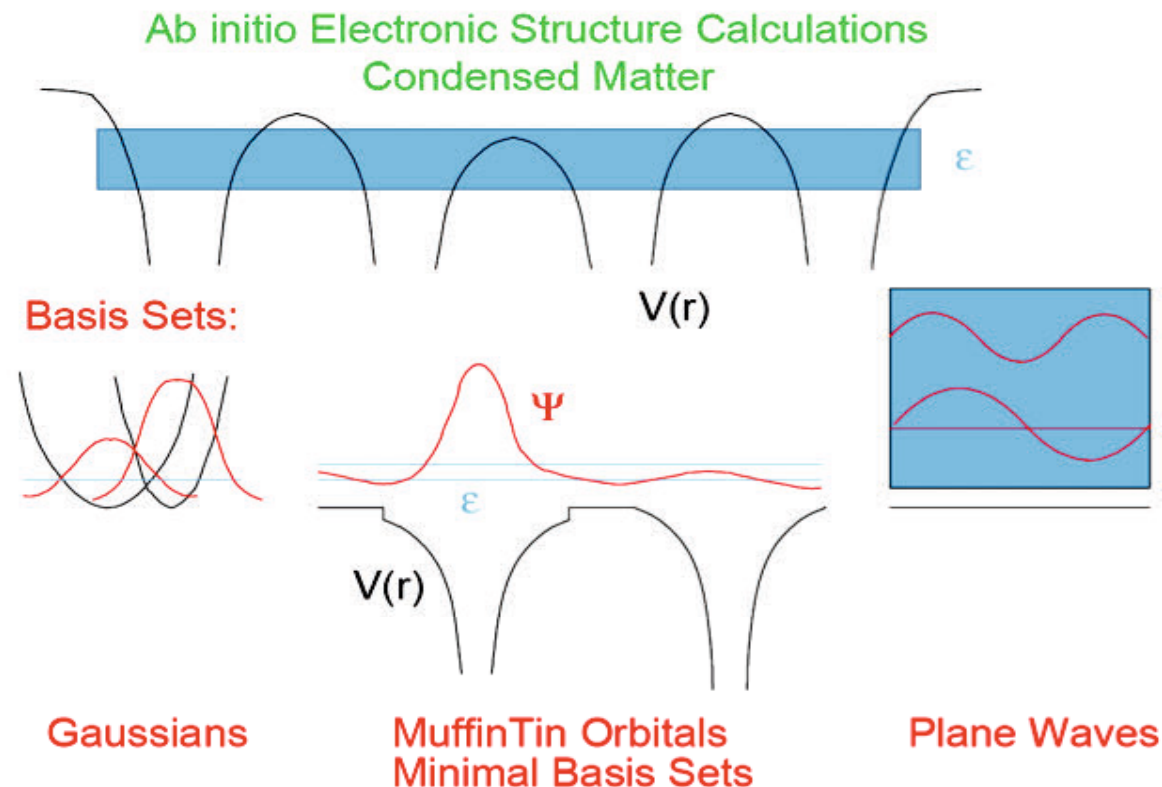
Max-Planck Institute for Solid-State Research, Stuttgart

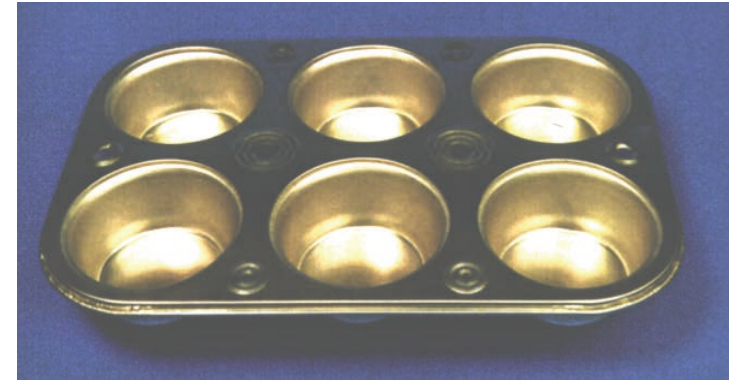
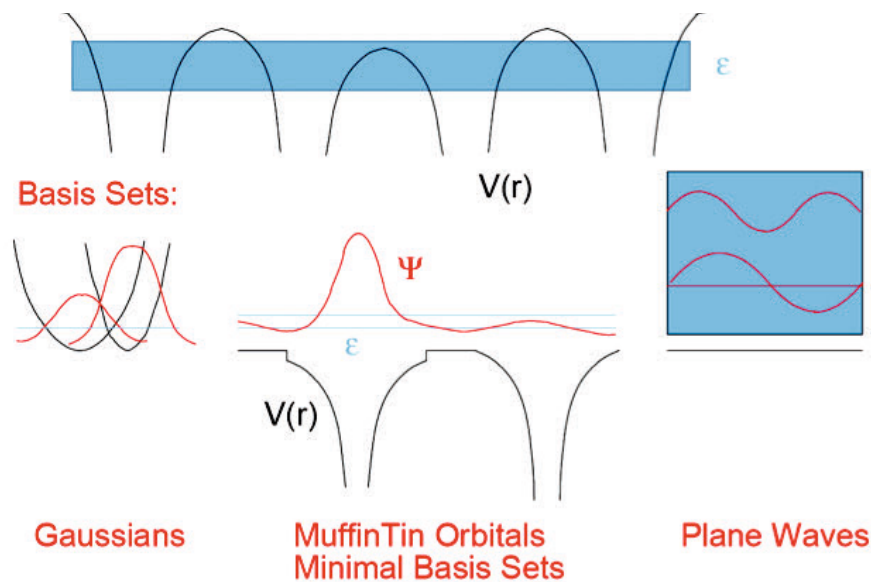
**One-electron basis sets for computation,
analysis and understanding**



1 Introduction

The electronic structure of condensed matter is usually described in terms of one-electron *basis sets*. Basis functions used for computation, or rather, their envelopes are usually mathematically simple functions, plane waves or Gaussians, in particular. A plane wave is a solution of Schrödinger's equation for a flat potential, and products of plane waves are plane waves; as a result, the charge density and its Hartree potential are plane-waves as well. Similarly, a Gaussian is a solution of Schrödinger's equation for a parabolically increasing potential, products of Gaussians are Gaussians, and the Hartree potential for a Gaussian charge density is $1/r$ times the error function. However, in order for such sets to give accurate results, the number of basis functions must be orders of magnitude larger than the number of valence electrons to be described.





By virtue of solving Schrödinger's equation for a muffin-tin well, the classical linear muffin-tin orbitals (LMTOs) [3, 4] form a comparatively small basis set. But only in the atomic-spheres approximation (ASA) where the MTOs are expanded in partial waves inside atomic spheres, assumed to fill space, do the products $\varphi_l(\epsilon, r) Y_{lm}(\hat{\mathbf{r}}) \times \varphi_{\bar{l}}(\bar{\epsilon}, r) Y_{\bar{l}\bar{m}}^*(\hat{\mathbf{r}})$ have the same form, $f_{L'}(r) Y_{L'm'}(\hat{\mathbf{r}})$, as each factor, and this is what makes the LMTO-ASA method exceedingly fast. However, the ASA is only accurate when the atoms are at high-symmetry positions.

For many purposes it is therefore desirable to extract a *small set of intelligible, localized orbitals* spanning merely selected conduction and/or valence states. For instance, if we want to describe the bonding, we need a localized basis set which spans the occupied states only (bond orbitals). If we want to construct models which add interactions to the one-electron Hamiltonian, e.g. electron-electron repulsions, we need a basis set of localized, atomic-like orbitals which describes the one-electron energies and wave functions in a suitable region around the Fermi level.

For an isolated set of energy bands in a *crystal*, $\varepsilon_i(\mathbf{k})$ ($i = 1, \dots, A$), this can be done by projecting from their delocalized Bloch eigenstates, $\Psi_i(\mathbf{k}; \mathbf{r})$ ($i = 1, \dots, A$) computed with the large basis set, a suitable set of generalized *Wannier functions*, $w_a(\mathbf{r} - \mathbf{t})$. These are enumerated by a ($= 1, \dots, A$) and the lattice translations, \mathbf{t} , of which there are $N \rightarrow \infty$, and they form a set of orthonormal functions related to the orthonormal Bloch eigenstates by a unitary transformation:

$$\Psi_i(\mathbf{k}; \mathbf{r}) = N^{-\frac{1}{2}} \sum_{\mathbf{t}} \sum_{a=1}^A u_{ia} \exp(i\mathbf{k} \cdot \mathbf{t}) w_a(\mathbf{r} - \mathbf{t}), \quad (1)$$

The inverse transformation:

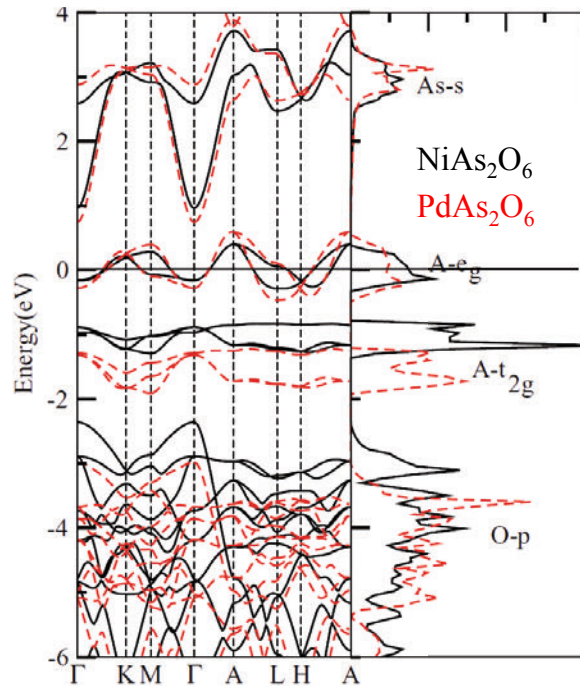
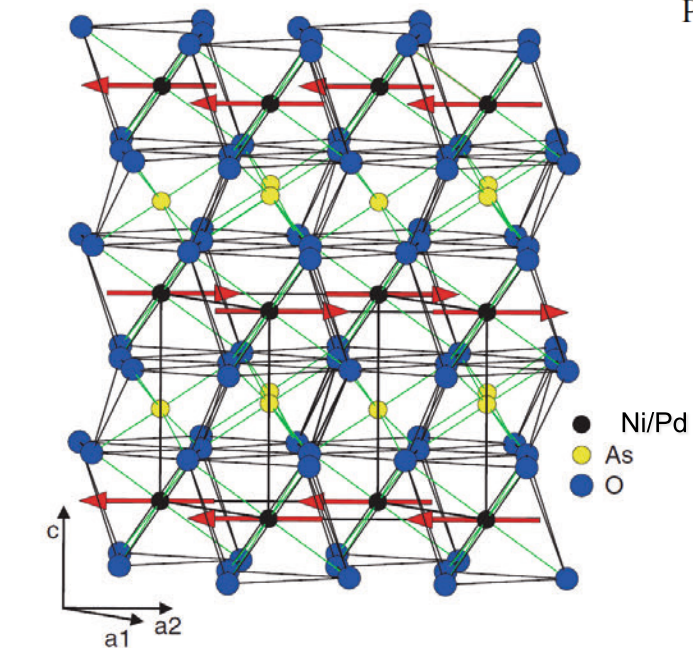
$$w_a(\mathbf{r} - \mathbf{t}) = N^{-\frac{1}{2}} \sum_{\mathbf{k}} \sum_{i=1}^A u_{ai}^* \exp(-i\mathbf{k} \cdot \mathbf{t}) \Psi_i(\mathbf{k}; \mathbf{r}), \quad (2)$$

is the Wannier projection. Wannier functions are not unique, because performing a unitary transformation, $W_{a\bar{a};\mathbf{t}-\mathbf{t}'}$, of one set of Wannier functions produces another set which also satisfies Eq. (1), merely with different i and \mathbf{k} -dependent phases of the Bloch functions. So the art of Wannier projection from the Bloch states (2) is to choose the i and \mathbf{k} -dependent phases of the latter in such a way that the Wannier functions attain desired properties, in particular optimal localization – in some sense. Mazari and Vanderbilt chose to minimize the spread $\langle w | |\mathbf{r} - \langle w | \mathbf{r} | w \rangle|^2 | w \rangle$ and developed an – otherwise general – numerical procedure for projecting such “maximally localized” Wannier functions from Bloch states expanded in plane waves [5].

$$w_a(\mathbf{r} - \mathbf{t}) = N^{-\frac{1}{2}} \sum_{\mathbf{k}} \sum_{i=1}^A u_{ai}^* \exp(-i\mathbf{k} \cdot \mathbf{t}) \Psi_i(\mathbf{k}; \mathbf{r}), \quad (2)$$

We shall only be interested in generating localized Wannier functions which resemble atomic orbitals, so-called *Wannier orbitals*, or simple linear combinations hereof such as bond orbitals. In this case, it is obvious that the phases in the projection (2) should be chosen such that when summing the Bloch states over i and \mathbf{k} , the atomic-orbital characters chosen for the Wannier functions should add up constructively. How localized the resulting Wannier orbitals are, then depends on how well the set of A bands are described by the characters chosen. This procedure was applied –presumably for the first time– by Satpathy and Pawłowska [6] to compute the sp^3 bond orbital in Si. They used the TB-LMTO basis [4] which makes the procedure quite obvious because the LMTO expansion has the same form as the expansion (2) in terms of Wannier functions, except that the unitary $A \times A$ matrix u_{ia} is replaced by the rectangular $A \times (A + P)$ matrix of LMTO eigenvectors. The projection is thus seen to be a *downfolding* in which each Wannier orbital becomes an *active* LMTO dressed by a tail of all the *passive* (P) LMTOs not in the set of active (A) ones. With other local-orbital basis sets, somewhat similar techniques can be used, but unless all basis functions are well localized, the Wannier orbitals obtained may not be sufficiently localized. For a further discussion we refer to last year’s lecture notes by Kunes [7].

For molecules, Boys [8] had a long time ago recognized that chemical bonds should be associated with those linear combinations of the occupied molecular orbitals which are most localized, because those linear combinations are most invariant to the surroundings.



$$J_{ij} \approx (t_{ij})^2 / U$$

FIG. 6. (Color online) The $x^2 - y^2$ (left panel) and $3z^2 - r^2$ (right panel) Wannier orbitals, which span the LDA Pd e_g bands of PdAs₂O₆. Plotted are orbital shapes (constant-amplitude surfaces) with lobes of opposite signs colored red (dark) and blue (light). For clarity, the central PdO₆ octahedron is given a blue skin and all AsO₆ octahedra a red skin. Pd atoms are green, As atoms are yellow, and O atoms are violet.

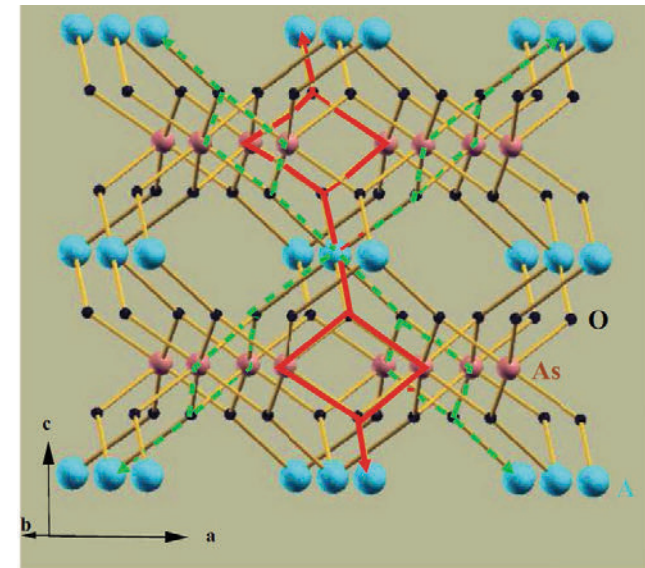
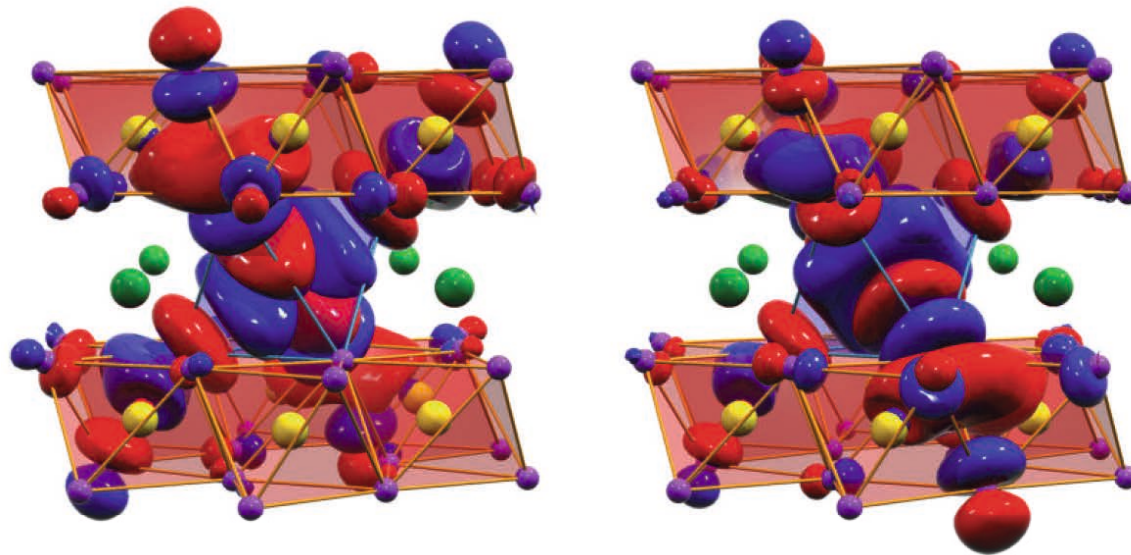
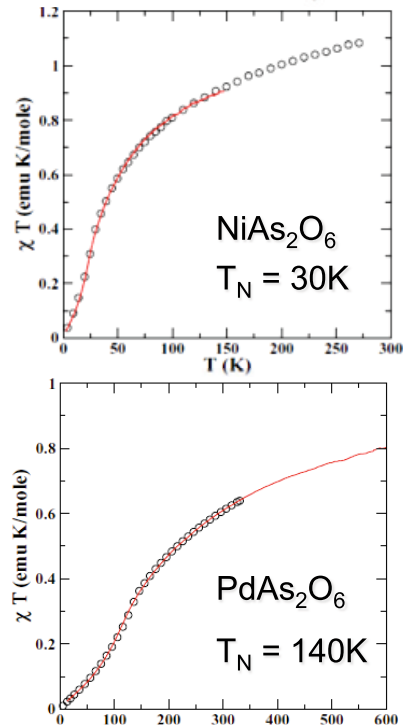


FIG. 7. (Color online) Paths of the dominant hoppings. Dashed green: between $x^2 - y^2$ orbitals (see the left-hand side of Fig. 6) on third-nearest A neighbors. Solid red: between $3z^2 - r^2$ orbitals (see the right-hand side of Fig. 6) on third-nearest A neighbors. The colors

The present notes deal with a different kind of basis set, specifically with minimal bases of N th-order muffin-tin orbitals (NMTOs), also known as 3rd generation MTOs [9–13]. We shall demonstrate that with NMTOs it is possible to generate Wannier functions *directly*, instead of via projection from the delocalized Bloch states. NMTOs are constructed from the partial-wave solutions of Schrödinger's equation for a superposition of *overlapping* spherical potential wells (muffin tins, MTs) [14, 15] and NMTO sets are therefore selective in energy. As a consequence, one can construct an NMTO set which picks a specific set of isolated energy bands. Since NMTOs are atom-centered and localized by construction, they do –after symmetric orthonormalization– form a set of localized Wannier functions which, if needed, can be recombined locally to have maximal localization. The NMTO technique is primarily for generating a *localized, minimal basis set with specific orbital characters*, and it can therefore be used also to pick a set of bands which overlap other bands outside the energy region of interest [16]. The corresponding NMTOs –orthonormalized or not– we refer to as Wannier-like. Once a computationally efficient representation is implemented for products of NMTOs [17], they should be suitable for full-potential, real-space calculations with a computational effort increasing merely linearly with the size (N) of the system, so-called order- N calculations [18, 19].

Model: Materials are made of atoms, and atoms are round

Periodic Table, with the Outer Electron Configurations of Neutral Atoms in Their Ground States

The notation used to describe the electronic configuration of atoms and ions is discussed in all textbooks of introductory atomic physics. The letters *s*, *p*, *d*, ... signify electrons having orbital angular momentum 0, 1, 2, ... in units \hbar ; the number to the left of the letter denotes the principal quantum number of one orbit, and the superscript to the right denotes the number of electrons in the orbit.

Li³ 2s	Be⁴ 2s ²											B⁵ 2s ² 2p	C⁶ 2s ² 2p ²	N⁷ 2s ² 2p ³	O⁸ 2s ² 2p ⁴	F⁹ 2s ² 2p ⁵	Ne¹⁰ 2s ² 2p ⁶																												
Na¹¹ 3s	Mg¹² 3s ²											Al¹³ 3s ² 3p	Si¹⁴ 3s ² 3p ²	P¹⁵ 3s ² 3p ³	S¹⁶ 3s ² 3p ⁴	Cl¹⁷ 3s ² 3p ⁵	Ar¹⁸ 3s ² 3p ⁶																												
K¹⁹ 4s	Ca²⁰ 4s ²	Sc²¹ 3d 4s ²	Ti²² 3d ² 4s ²	V²³ 3d ³ 4s ²	Cr²⁴ 3d ⁵ 4s	Mn²⁵ 3d ⁵ 4s ²	Fe²⁶ 3d ⁶ 4s ²	Co²⁷ 3d ⁷ 4s ²	Ni²⁸ 3d ⁸ 4s ²	Cu²⁹ 3d ¹⁰ 4s	Zn³⁰ 3d ¹⁰ 4s ²	Ga³¹ 4s ² 4p	Ge³² 4s ² 4p ²	As³³ 4s ² 4p ³	Se³⁴ 4s ² 4p ⁴	Br³⁵ 4s ² 4p ⁵	Kr³⁶ 4s ² 4p ⁶																												
Rb³⁷ 5s	Sr³⁸ 5s ²	Y³⁹ 4d 5s ²	Zr⁴⁰ 4d ² 5s ²	Nb⁴¹ 4d ⁴ 5s	Mo⁴² 4d ⁵ 5s	Tc⁴³ 4d ⁶ 5s	Ru⁴⁴ 4d ⁷ 5s	Rh⁴⁵ 4d ⁸ 5s	Pd⁴⁶ 4d ¹⁰ -	Ag⁴⁷ 4d ¹⁰ 5s	Cd⁴⁸ 4d ¹⁰ 5s ²	In⁴⁹ 5s ² 5p	Sn⁵⁰ 5s ² 5p ²	Sb⁵¹ 5s ² 5p ³	Te⁵² 5s ² 5p ⁴	I⁵³ 5s ² 5p ⁵	Xe⁵⁴ 5s ² 5p ⁶																												
Cs⁵⁵ 6s	Ba⁵⁶ 6s ²	La⁵⁷ 5d 6s ²	Hf⁷² 4f ¹⁴ 5d ² 6s ²	Ta⁷³ 5d ³ 6s ²	W⁷⁴ 5d ⁴ 6s ²	Re⁷⁵ 5d ⁵ 6s ²	Os⁷⁶ 5d ⁶ 6s ²	Ir⁷⁷ 5d ⁹ -	Pt⁷⁸ 5d ⁹ 6s	Au⁷⁹ 5d ¹⁰ 6s	Hg⁸⁰ 5d ¹⁰ 6s ²	Tl⁸¹ 6s ² 6p	Pb⁸² 6s ² 6p ²	Bi⁸³ 6s ² 6p ³	Po⁸⁴ 6s ² 6p ⁴	At⁸⁵ 6s ² 6p ⁵	Rn⁸⁶ 6s ² 6p ⁶																												
Fr⁸⁷ 7s	Ra⁸⁸ 7s ²	Ac⁸⁹ 6d 7s ²	<table border="1"> <tr> <td>Ce⁵⁸ 4f² 6s²</td> <td>Pr⁵⁹ 4f³ 6s²</td> <td>Nd⁶⁰ 4f⁴ 6s²</td> <td>Pm⁶¹ 4f⁵ 6s²</td> <td>Sm⁶² 4f⁶ 6s²</td> <td>Eu⁶³ 4f⁷ 6s²</td> <td>Gd⁶⁴ 4f⁷ 5d 6s²</td> <td>Tb⁶⁵ 4f⁸ 5d 6s²</td> <td>Dy⁶⁶ 4f¹⁰ 6s²</td> <td>Ho⁶⁷ 4f¹¹ 6s²</td> <td>Er⁶⁸ 4f¹² 6s²</td> <td>Tm⁶⁹ 4f¹³ 6s²</td> <td>Yb⁷⁰ 4f¹⁴ 6s²</td> <td>Lu⁷¹ 4f¹⁴ 5d 6s²</td> </tr> <tr> <td>Th⁹⁰ - 6d² 7s²</td> <td>Pa⁹¹ 5f² 6d 7s²</td> <td>U⁹² 5f³ 6d 7s²</td> <td>Np⁹³ 5f⁴ 7s²</td> <td>Pu⁹⁴ 5f⁶ 7s²</td> <td>Am⁹⁵ 5f⁷ 7s²</td> <td>Cm⁹⁶ 5f⁷ 6d 7s²</td> <td>Bk⁹⁷</td> <td>Cf⁹⁸</td> <td>Es⁹⁹</td> <td>Fm¹⁰⁰</td> <td>Md¹⁰¹</td> <td></td> <td>Lw¹⁰³</td> </tr> </table>															Ce⁵⁸ 4f ² 6s ²	Pr⁵⁹ 4f ³ 6s ²	Nd⁶⁰ 4f ⁴ 6s ²	Pm⁶¹ 4f ⁵ 6s ²	Sm⁶² 4f ⁶ 6s ²	Eu⁶³ 4f ⁷ 6s ²	Gd⁶⁴ 4f ⁷ 5d 6s ²	Tb⁶⁵ 4f ⁸ 5d 6s ²	Dy⁶⁶ 4f ¹⁰ 6s ²	Ho⁶⁷ 4f ¹¹ 6s ²	Er⁶⁸ 4f ¹² 6s ²	Tm⁶⁹ 4f ¹³ 6s ²	Yb⁷⁰ 4f ¹⁴ 6s ²	Lu⁷¹ 4f ¹⁴ 5d 6s ²	Th⁹⁰ - 6d ² 7s ²	Pa⁹¹ 5f ² 6d 7s ²	U⁹² 5f ³ 6d 7s ²	Np⁹³ 5f ⁴ 7s ²	Pu⁹⁴ 5f ⁶ 7s ²	Am⁹⁵ 5f ⁷ 7s ²	Cm⁹⁶ 5f ⁷ 6d 7s ²	Bk⁹⁷	Cf⁹⁸	Es⁹⁹	Fm¹⁰⁰	Md¹⁰¹		Lw¹⁰³
Ce⁵⁸ 4f ² 6s ²	Pr⁵⁹ 4f ³ 6s ²	Nd⁶⁰ 4f ⁴ 6s ²	Pm⁶¹ 4f ⁵ 6s ²	Sm⁶² 4f ⁶ 6s ²	Eu⁶³ 4f ⁷ 6s ²	Gd⁶⁴ 4f ⁷ 5d 6s ²	Tb⁶⁵ 4f ⁸ 5d 6s ²	Dy⁶⁶ 4f ¹⁰ 6s ²	Ho⁶⁷ 4f ¹¹ 6s ²	Er⁶⁸ 4f ¹² 6s ²	Tm⁶⁹ 4f ¹³ 6s ²	Yb⁷⁰ 4f ¹⁴ 6s ²	Lu⁷¹ 4f ¹⁴ 5d 6s ²																																
Th⁹⁰ - 6d ² 7s ²	Pa⁹¹ 5f ² 6d 7s ²	U⁹² 5f ³ 6d 7s ²	Np⁹³ 5f ⁴ 7s ²	Pu⁹⁴ 5f ⁶ 7s ²	Am⁹⁵ 5f ⁷ 7s ²	Cm⁹⁶ 5f ⁷ 6d 7s ²	Bk⁹⁷	Cf⁹⁸	Es⁹⁹	Fm¹⁰⁰	Md¹⁰¹		Lw¹⁰³																																

Atomic number
=
number of protons in the nucleus
=
number of electrons in the neutral atom

configuration of outer shells in the ground state of the neutral atom

One step to the right adds one positively charged proton (and a neutron) to the nucleus and this attracts one more negatively charged electron to the atomic shell.

2 The idea

The idea behind linear basis sets can be understood by considering first how Wigner and Seitz thought about solving the one-electron eigenvalue problem in a solid; in case of a crystal, that is the band-structure problem. They divided space into atom-centered cells and assumed the potential to be spherically symmetric inside each cell,

$$V(\mathbf{r}) = \sum_R v_R(r_R).$$

Here and in the following, $r_R \equiv |\mathbf{r} - \mathbf{R}|$, and R labels the sites, \mathbf{R} . With this approximation, Schrödinger's equation (in atomic Rydberg units),

$$[\mathcal{H} - \varepsilon] \Psi(\varepsilon, \mathbf{r}) = [-\nabla^2 + V(\mathbf{r}) - \varepsilon] \Psi(\varepsilon, \mathbf{r}) = 0,$$

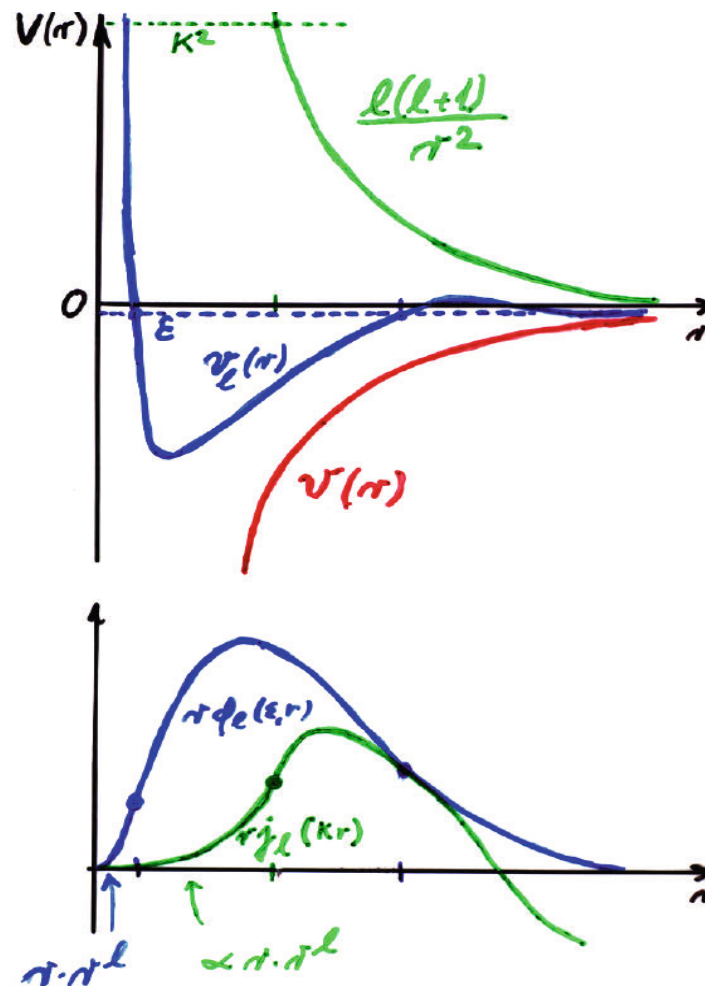
can be treated as a separable differential equation: The eigenfunctions must have a *partial-wave expansion* inside each cell,

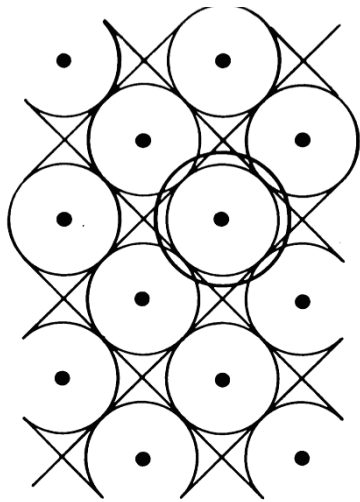
$$\Psi(\varepsilon, \mathbf{r}) = \sum_{lm} \varphi_{Rl}(\varepsilon, r_R) Y_{lm}(\hat{\mathbf{r}}_R) c_{Rlm},$$

and one may therefore proceed by first solving the *radial* Schrödinger equations,

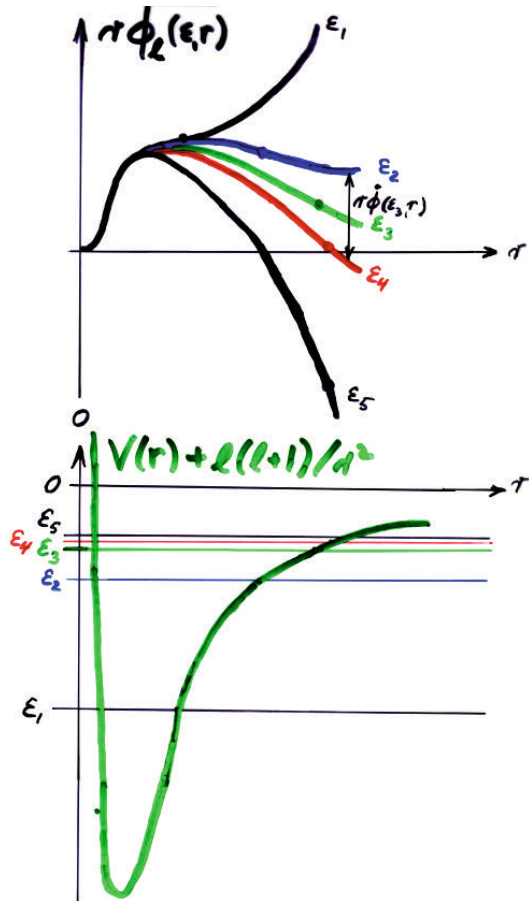
$$\left[\frac{\partial^2}{\partial r^2} + \varepsilon - v_R(r) - \frac{l(l+1)}{r^2} \right] r\varphi_{Rl}(\varepsilon, r) = 0,$$

for all R and l and a given energy, ε , and then seek coefficients, c_{Rlm} , for which the partial-wave expansions join together continuously and differentiably at the cell boundaries. The energies for which this is possible are the eigenvalues, $\varepsilon = \varepsilon_i$, and $\Psi_i(\varepsilon_i, \mathbf{r})$ the eigenfunctions.





Crystal structure



This point of view for instance leads to the *approximate* Wigner-Seitz rules stating that for an elemental, close-packed crystal, where the cell can be substituted by an atomic sphere of the same volume ($\Omega = 4\pi w^3/3$), a band of l -character exists between the energies ϵ_{lB} and ϵ_{lA} for which respectively the slope and the value of $\varphi_l(\epsilon, r)$ vanishes at the atomic sphere. These band edges correspond to the bonding and antibonding states of a homonuclear diatomic molecule. In the atomic-spheres approximation (ASA), the input to the band structure from the potential enters exclusively via the dimensionless, *radial logarithmic derivative functions* evaluated at the sphere,

$$D\{\varphi_l(\epsilon, w)\} \equiv \partial \ln |\varphi_l(\epsilon, r)| / \partial \ln r|_w.$$

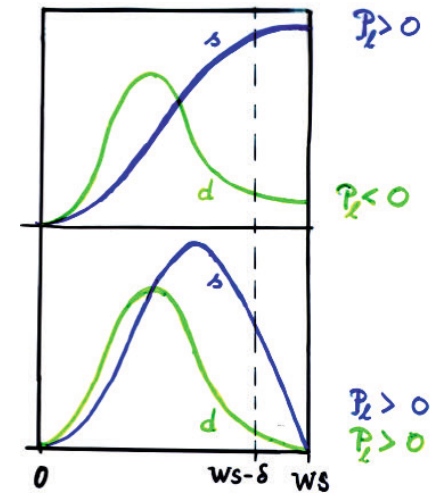
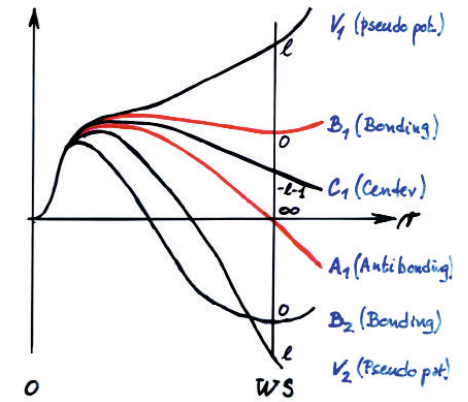
These are ever decreasing functions of energy, and the bonding/antibonding boundary condition is:

$$D\{\varphi_l(\epsilon, w)\} = 0/\infty.$$

To set up the matching problem correctly in a direct way, however, makes it necessary to deal with cells rather than spheres, and with *all* the partial waves required to make the one-center expansion,

$$\sum_{lm} \varphi_{Rl}(\epsilon, r_R) Y_{lm}(\hat{r}_R) c_{Rlm},$$

converged at the cell-boundary. This takes $l \lesssim 15$ and is not practical.



Next, consider the customary and more general way of solving Schrödinger's equation, namely by use of the Raleigh-Ritz variational principle for the Hamiltonian with a trial function expressed as a superposition of basis functions, $\chi_g(\mathbf{r})$,

$$\Psi(\mathbf{r}) \approx \sum_g \chi_g(\mathbf{r}) b_g.$$

Variation of the coefficients b_g leads to the algebraic, generalized eigenvalue problem:

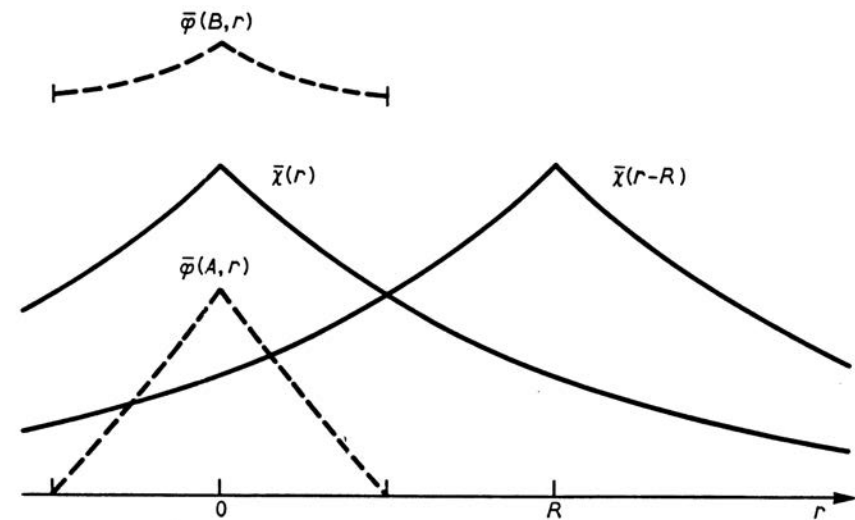
$$\sum_g \left(\langle \chi_{\bar{g}} | \mathcal{H} | \chi_g \rangle - \varepsilon \langle \chi_{\bar{g}} | \chi_g \rangle \right) b_g = 0,$$

for all \bar{g} , in terms of Hamiltonian and overlap matrices, $\langle \chi | \mathcal{H} | \chi \rangle$ and $\langle \chi | \chi \rangle$. The eigenvalues, ε_i , are variational estimates of the one-electron energies, and the eigenvectors, $b_{g,i}$, give the wavefunctions $\Psi_i(\mathbf{r})$. The problem with this approach is to devise efficient basis sets.

The idea is now to construct the basis set in such a way that for the approximate model potential, $\sum_R v_R(r_R)$, the set solves Schrödinger's equation exactly to linear order in the deviation of the eigenvalue from an energy, ε_ν , chosen at the center of interest, i.e. such that the error is

$$\Psi_i(\mathbf{r}) - \Psi_i(\varepsilon_i, \mathbf{r}) \propto (\varepsilon_i - \varepsilon_\nu)^2.$$

By virtue of the variational principle, the errors of the eigenvalues will then be of order $(\varepsilon_i - \varepsilon_\nu)^4$. Imagine what such linear basis functions must look like if we choose them as atom-centered orbitals, $\chi_{Rlm}(\mathbf{r}_R)$:



Bonding and antibonding states of a diatomic molecule.

In order that the linear combination $\sum_g \chi_g(\mathbf{r}) b_g$ be able to provide the correct eigenfunctions,

$$\Psi(\varepsilon, \mathbf{r}) = \sum_{lm} \varphi_{Rl}(\varepsilon, r_R) Y_{lm}(\hat{\mathbf{r}}_R) c_{Rlm},$$

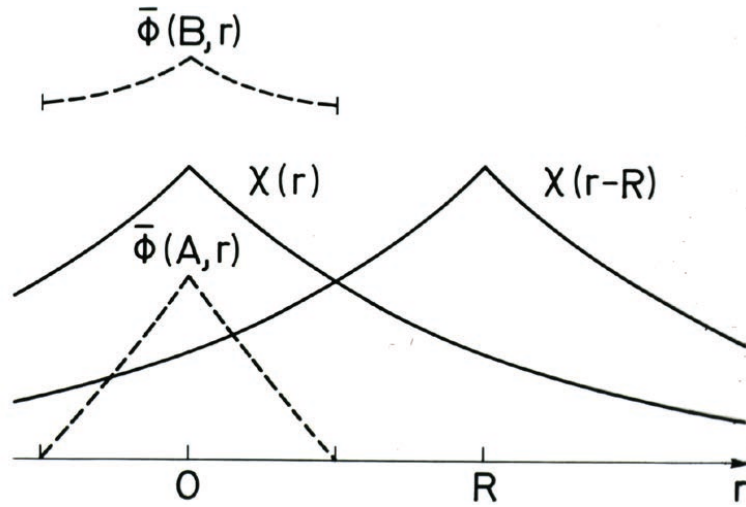
for a spectrum of eigenvalues, ε_i , near ε_ν , the *tails* of the orbitals entering a particular cell (R) must, when expanded in spherical harmonics around \mathbf{R} , have radial parts which are *energy-derivative functions*:

$$\dot{\varphi}_{Rl}(\varepsilon_\nu, r_R) \equiv \partial \varphi_{Rl}(\varepsilon, r_R) / \partial \varepsilon |_{\varepsilon_\nu},$$

because then, the sum of the tails added to the head of the orbital will be able to yield the result

$$\varphi_{Rl}(\varepsilon_\nu, r_R) + (\varepsilon_i - \varepsilon_\nu) \dot{\varphi}_{Rl}(\varepsilon_\nu, r_R) = \varphi_{Rl}(\varepsilon_i, r_R) + O((\varepsilon_i - \varepsilon_\nu)^2).$$

Hence, the radial shape of a *head* must be $\varphi_{Rl}(\varepsilon_\nu, r_R)$, plus maybe a bit of $\dot{\varphi}_{Rl}(\varepsilon_\nu, r_R)$.



$$\chi_{RL}(\mathbf{r}_R) = \phi_{RL}(\epsilon_\nu, \mathbf{r}_R) + \sum_{R'L'} \dot{\phi}_{R'L'}(\epsilon_\nu, \mathbf{r}_R) (H_{R'L', RL} - \epsilon_\nu \delta_{R'L', RL})$$

with $L \equiv lm$. In order to show explicitly how the solutions of the Schrödinger equation for the solid can be described through overlap of orbitals, we may simply diagonalize H . Naming its eigenvectors and eigenvalues respectively $u_{RL,i}$ and ϵ_i , the linear combination of orbitals given by an eigenvector is:

$$\begin{aligned} |\chi\rangle u_i &= [|\phi\rangle + |\dot{\phi}\rangle (H - \epsilon_\nu)] u_i \\ &= [|\phi\rangle + |\dot{\phi}\rangle (\epsilon_i - \epsilon_\nu)] u_i \\ &= |\phi(\epsilon_i)\rangle u_i + O((\epsilon_i - \epsilon_\nu)^2), \end{aligned}$$

as anticipated. LMTOs thus naturally describe the way in which the overlap of orbitals leads to broadening of levels into bands.

The condition that the spherical-harmonics expansion of the tail around site R have the radial behavior $\dot{\phi}_{Rl}(\epsilon_\nu, r_R)$ for all lm and all R , might seem to determine the shape of the orbital completely and not even allow it to be smooth, but merely continuous. However, adding φ to $\dot{\phi}$ yields another $\dot{\phi}$, corresponding to a different energy-dependent normalization, e.g.

$$\frac{\partial}{\partial \epsilon} [1 + (\epsilon - \epsilon_\nu) o] \varphi(\epsilon, r) \Big|_{\epsilon_\nu} = \dot{\phi}(\epsilon_\nu, r) + o \varphi(\epsilon_\nu, r).$$

Hence, $\dot{\phi}_{Rl}(\epsilon_\nu, r)$ can be adjusted to have, say, a required value and slope at some radius, a_R , where a linear combination, $\sum_{lm} \dot{\phi}_{Rl}(\epsilon_\nu, r_R) Y_{lm}(\hat{\mathbf{r}}_R)$, can then be matched smoothly onto any given orbital shape

More practical than matching the partial waves at the cell boundaries, it is therefore to embed the partial waves in a set of *envelope functions* or, from the point of view of the latter, to *augment* the envelope functions with partial waves. In order that the one-center expansions $\sum_{lm} \varphi_{Rl}(\epsilon, r_R) Y_{lm}(\hat{\mathbf{r}}_R) c_{Rlm}$ converge in l , the envelope functions must be such that they match $\varphi_{Rl}(\epsilon, r_R)$ for high l , whereby augmentation of the high- l waves becomes unnecessary, as long as they are taken into account as the high- l part of the envelopes. As l increases, the centrifugal term $l(l+1)/r^2$ of the radial Schrödinger equation drives $\varphi_{Rl}(\epsilon, r)$ outwards such that eventually only the outermost, flat part of the potential is being felt.

At that point,

$$\varphi_{Rl}(\varepsilon, r) \rightarrow j_l(r\kappa_R) \rightarrow \text{const.} \times r^l,$$

where $\kappa_R^2 \equiv \varepsilon - v_R(s_R)$. Acceptable envelope functions are therefore solutions of the *wave equation*,

$$[\nabla^2 + \kappa^2] h(\varepsilon, \mathbf{r}) = 0,$$

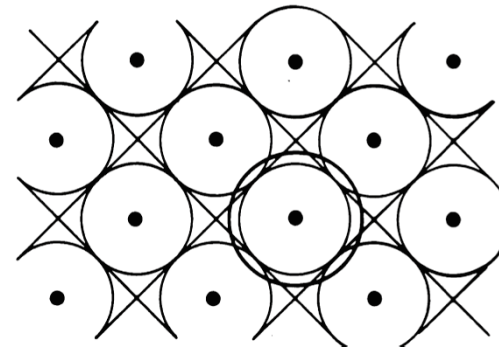
with energies $\kappa^2 \sim \varepsilon$, where the zero of potential is taken as the average between the atoms. *Spherical waves* are used for muffin-tin orbitals (MTOs) and *plane waves* are used for APWs. Gaussians do not seem suitable because they are Schrödinger solutions for a parabolically increasing, rather than a flat potential.

For all augmented basis sets, the model potential is a *superposition of spherically symmetric potential wells*, but their range, s_R , varies. APWs and LMTOs used in full-potential calculations employ muffin-tin potentials with non-overlapping spheres. For open structures, empty spheres –i.e. without nuclei– are included at interstitial sites. Owing to its sizeable remaining interstitial region ($\sim 0.3\Omega$) and strong discontinuities at the spheres, such a MT-potential remains a bad approximation to the full potential, whose matrix elements must therefore be included in the Hamiltonian. Nevertheless, such a basis is not optimal and –whenever possible– one uses potential spheres with

a positive radial overlap,

$$\omega_{R\bar{R}}^s \equiv \frac{s_R + s_{\bar{R}}}{|\mathbf{R} - \bar{\mathbf{R}}|} - 1,$$

of up to 20%, and neglects the associated errors. For exact, energy dependent MTOs with $\kappa^2 = \varepsilon$ (EMTOs), these errors turn out to be merely of 2nd order in the potential overlap and, as a consequence, EMTOs can handle up to 50% overlap. Another solution to this problem is offered by the so-called smooth Hankel functions devised by Methfessel and Schilfgaard.



With EMTOs it is possible to construct not only energy-independent *linear* basis sets, but also basis sets of *arbitrary order* without increasing the size of the set. Specifically, for a mesh of $N + 1$ energies, $\varepsilon_0, \dots, \varepsilon_N$, a basis set of N th order will span the solutions of Schrödinger's equation for the model potential with the error

$$\Psi_i(\mathbf{r}) - \Psi_i(\varepsilon_i, \mathbf{r}) \propto (\varepsilon_i - \varepsilon_0)(\varepsilon_i - \varepsilon_1) \dots (\varepsilon_i - \varepsilon_N).$$

Since distances between close-packed spheres are small compared with the shortest wavelength $2\pi/\kappa_F$ of the valence electrons, the κ^2 dependence of the spherical waves (12) is of far less importance [27] than that of the ε dependence of the logarithmic derivatives (7). For that reason LMTOs of the 1st [22, 3] and 2nd [4] generations used $\kappa^2 \equiv 0$, thus simplifying the decaying Hankel functions to multipole potentials $\propto r^{-l-1}$, which got screened in the 2nd generation. With $\kappa \equiv 0$ and the ASA, the WS rules for the energies of the band edges in an elementary close-packed solid could be generalized to the unhybridized band structures, $\varepsilon_{li}(\mathbf{k}) = fct(D_l)$, the so-called canonical bands [22, 3, 23, 24, 26, 28].

Springer Series in
Solid-State Sciences 41

H.L.Skriver

The LMTO Method

Muffin-Tin Orbitals and Electronic Structure



Springer-Verlag
Berlin Heidelberg New York Tokyo

SOCIETÀ ITALIANA DI FISICA
RENDICONTI
DELLA
SCUOLA INTERNAZIONALE DI FISICA
«ENRICO FERMI»

LXXXIX CORSO

*Punti focali
nella teoria degli stati condensati*



SOCIETÀ ITALIANA DI FISICA BOLOGNA - ITALY

Lecture Notes in Physics

Edited by H. Araki, Kyoto, J. Ehlers, München, K. Hepp, Zürich
R. Kippenhahn, München, H.A. Weidenmüller, Heidelberg
J. Wess, Karlsruhe and J. Zittartz, Köln

283

M. Yussouff (Ed.)

Electronic Band Structure
and Its Applications

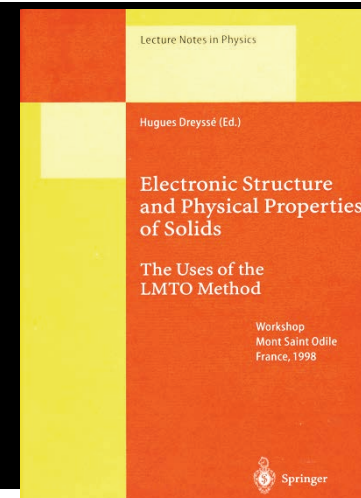
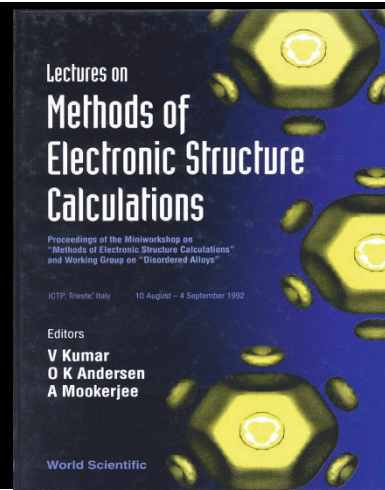
Proceedings, Kanpur, India 1986

For the exact, energy-dependent MTOs (EMTOs) [20] with $\kappa^2 = \varepsilon$, which we shall consider in the following section, the *overlap errors* turn out to be merely of 2nd order in the potential overlap [14] and, as a consequence, EMTOs can handle up to 50% overlap. The overlapping MT approximation (OMTA) is a least-squares fit to the full potential [14, 15] so that the MT discontinuities decrease with increasing overlap.

With EMTOs, also *downfolding* works perfectly [20], which was not the case with the old LMTOs [29]. However, with increasing downfolding, the range of the EMTOs and herewith their energy dependence increases. So it became necessary to construct not only energy-independent linear basis sets, but also basis sets of *arbitrary order* without increasing the size of the set. Specifically, for a mesh of $N + 1$ energies, $\varepsilon_0, \dots, \varepsilon_N$, a basis set of N th order will span the solutions of Schrödinger's equation for the model potential with the error

$$\Psi_i(\mathbf{r}) - \Psi_i(\varepsilon_i, \mathbf{r}) \propto (\varepsilon_i - \varepsilon_0)(\varepsilon_i - \varepsilon_1) \dots (\varepsilon_i - \varepsilon_N). \quad (14)$$

These are the so-called *NMTO* and *NAPW* basis sets, of which we shall consider the former.



3 Crystals

In the above, R runs over all atoms in the system. If it is a crystal with translations \mathbf{T} , the wave functions and the basis functions can be chosen to translate according to:

$$\Psi(\mathbf{r} + \mathbf{T}) = e^{i\mathbf{k}\cdot\mathbf{T}}\Psi(\mathbf{r}).$$

Orbitals can then be Bloch-summed:

$$\chi_{Rlm}^{\mathbf{k}}(\mathbf{r}) \equiv \sum_{\mathbf{T}} \chi_{Rlm}(\mathbf{r}_R - \mathbf{T}) e^{i\mathbf{k}\cdot\mathbf{T}},$$

where R now labels the atoms in the primitive cell. Rather than normalizing the Bloch sums over the entire crystal, we have normalized them in the primitive cell. Accordingly, $\sum_{\mathbf{k}}$ must be taken as the average, rather than the sum, over the Brillouin zone. Matrices like the Hamiltonian are translationally invariant,

$$\begin{aligned} \langle \chi_{\bar{R}\bar{l}\bar{m}}(\mathbf{r}_{\bar{R}}) | \mathcal{H} | \chi_{Rlm}(\mathbf{r}_R - \mathbf{T}) \rangle = \\ \langle \chi_{\bar{R}\bar{l}\bar{m}}(\mathbf{r}_{\bar{R}} + \mathbf{T}) | \mathcal{H} | \chi_{Rlm}(\mathbf{r}_R) \rangle, \end{aligned}$$

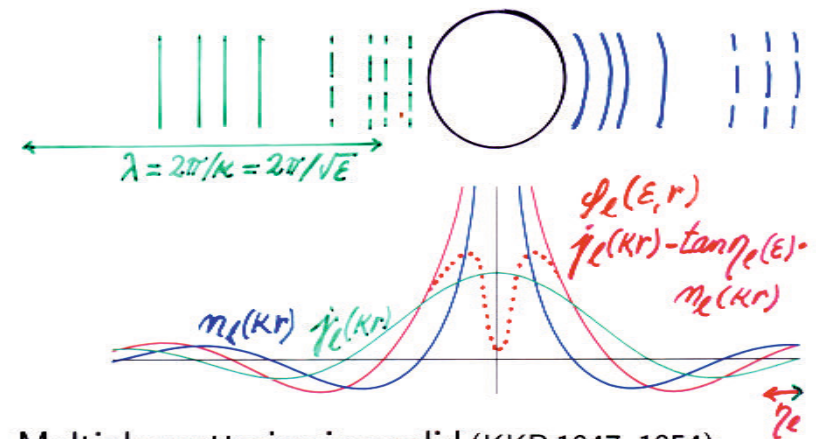
and as a consequence,

$$\begin{aligned} \langle \chi_{\bar{R}\bar{l}\bar{m}}^{\mathbf{k}}(\mathbf{r}) | \mathcal{H} | \chi_{Rlm}^{\mathbf{k}}(\mathbf{r}) \rangle \equiv \\ \sum_{\mathbf{T}} \langle \chi_{\bar{R}\bar{l}\bar{m}}(\mathbf{r}_{\bar{R}}) | \mathcal{H} | \chi_{Rlm}(\mathbf{r}_R - \mathbf{T}) \rangle e^{i\mathbf{k}\cdot\mathbf{T}}. \end{aligned}$$

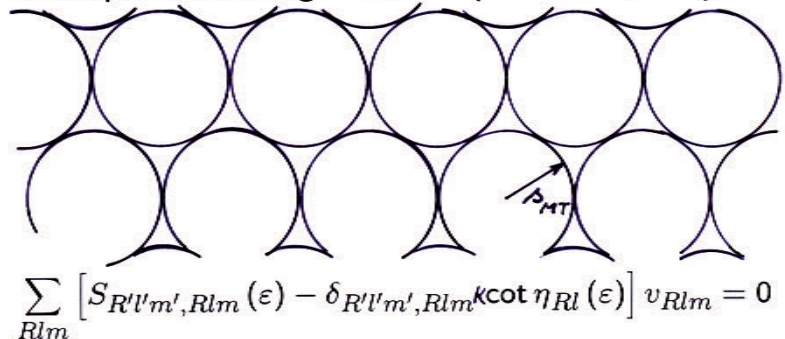
Numerical calculations are often carried out in the \mathbf{k} -representation, but since it is trivial to add superscripts \mathbf{k} and limit R to the sites in the primitive cell, in formalisms for orbitals it is simpler and more general to use the real-space representation.

4 Muffin-tin orbitals

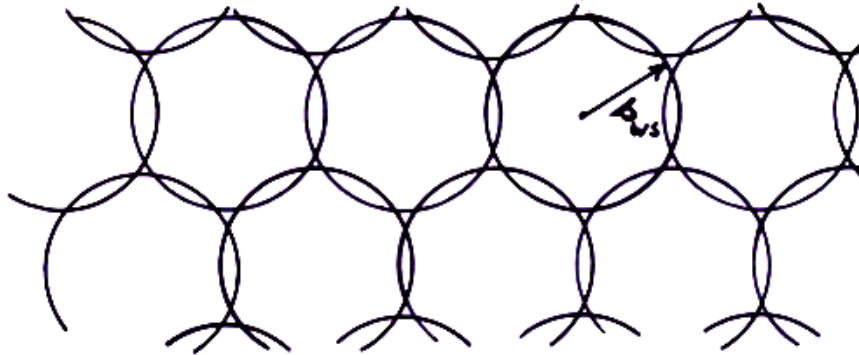
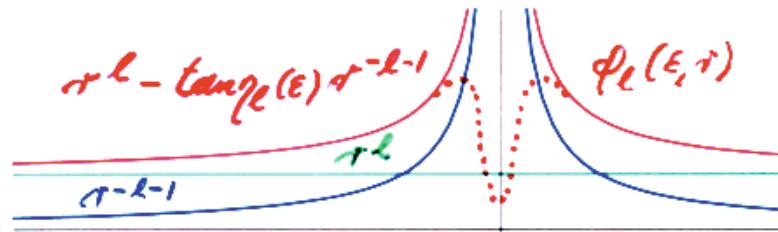
Elastic scattering from a single atom:



Multiple scattering in a solid (KKR 1947, 1954):

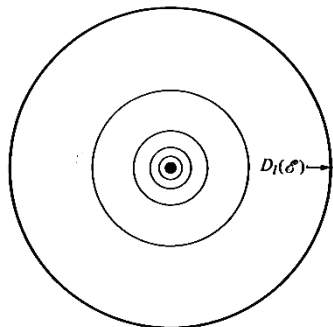


Atomic Spheres Approximation (1973): $\kappa \equiv 0$

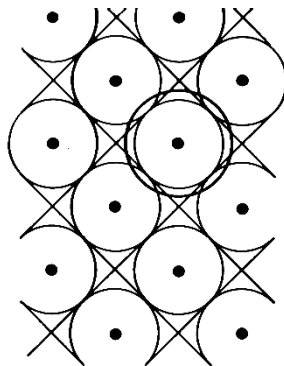


$$\sum_{RL} [S_{R'L',RL} - \delta_{R'L',RL} \cot \eta_{RL}(\epsilon)] v_{RL} = 0$$

$$\sum_L [S_{L'L}(\mathbf{k}) - \delta_{L'L} \cot \eta_L(\epsilon)] v_L = 0$$

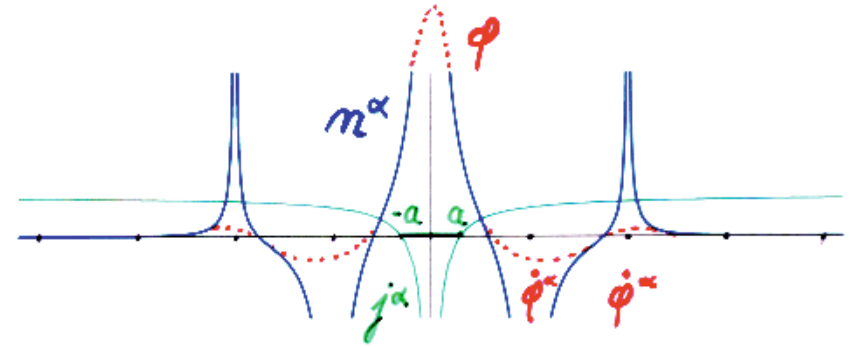


Atomic Wigner-Seitz sphere



Crystal structure

Screening \Rightarrow *Ab initio* TB-LMTO-ASA (1984):



$$n_{R'L'}^\alpha(\mathbf{r} - \mathbf{R}') \equiv \sum_{RL} n_L(\mathbf{r} - \mathbf{R}) [\delta_{RL,R'L'} + \tan \alpha_l S_{RL,R'L'}^\alpha]$$

$$j_l^\alpha(r) \equiv j_l(r) - \tan \alpha_l n_l(r)$$

$$(S^\alpha)_{RL,R'L'}^{-1} = (S^{-1})_{RL,R'L'} - \delta_{RL,R'L'} \tan \alpha_l$$

$$\tan \eta_l^\alpha(\epsilon) \equiv \tan \eta_l(\epsilon) - \tan \alpha_l$$

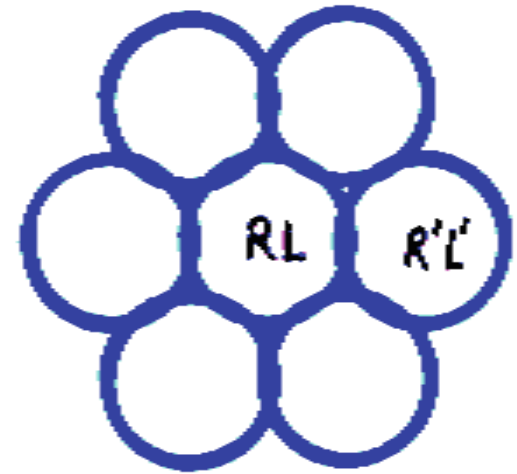
$$\sum_{RL} [S_{R'L',RL}^\alpha - \delta_{R'L',RL} \cot \eta_{RL}^\alpha(\epsilon)] v_{RL} = 0$$

Electronic structure of disordered condensed matter and extended defects.

$$\left(\frac{\Delta_l}{E - C_l} + \gamma_l \right) \leftarrow S_{l'm'; lm}(\bar{\mathbf{k}})$$

$$H = C + \sqrt{\Delta} S (1 - \gamma S)^{-1} \sqrt{\Delta}$$

$$S_{ss\sigma} = -2(s/R), \quad S_{sp\sigma} = 2\sqrt{3}(s/R)^2, \dots$$



Closely packed solid. ASA (1984):

Wave fct $\Psi_j(\mathbf{r}) = \sum_{Rlm} \phi_{Rl}(\varepsilon_j, \mathbf{r}_R) Y_{lm}(\hat{\mathbf{r}}_R) c_{Rlm,j}$

KKR $\sum_{RL} \left[S_{R'L',RL}^\alpha - P_{RL}^\alpha(\varepsilon_j) \delta_{R'L',RL} \right] c_{RL,j} = 0, \quad \text{for all } R'L'$

LMTO $\chi_{RL}^\alpha(\mathbf{r}_R) = \phi_{R'L'}(\varepsilon_\nu, \mathbf{r}_{R'}) \delta_{R'L',RL} + \dot{\phi}_{R'L'}^\alpha(\varepsilon_\nu, \mathbf{r}_{R'}) h_{R'L',RL}^\alpha$

in short $\chi_j = |o\rangle - |\dot{o}\rangle h, \quad 2c \text{ Hamiltonian: } h = \dot{P}^{-1/2} (S - P) \dot{P}^{-1/2}$

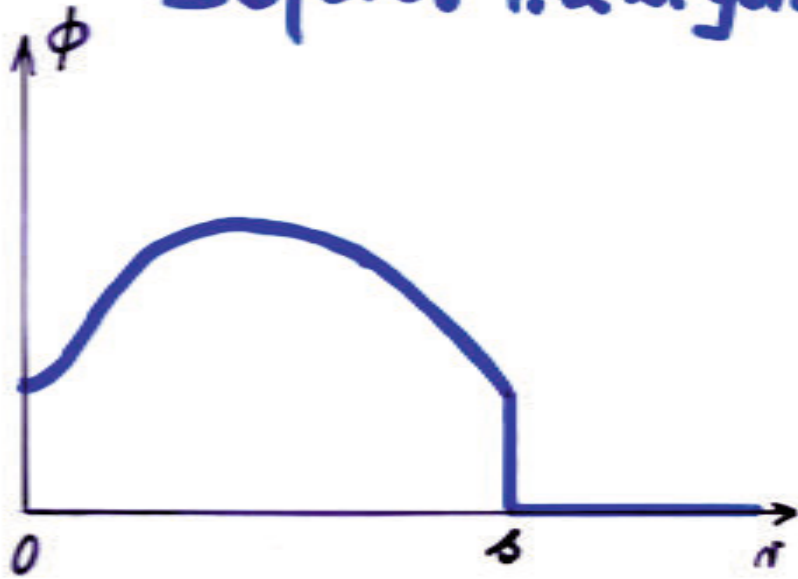
Eigenvalue eq $hc_j = (\varepsilon_j - \varepsilon_\nu) c_j$

Wave fct $\Psi_j = \chi_j c_j = \left[|o\rangle - |\dot{o}\rangle h \right] c_j = \left[|\dot{o}\rangle + \dot{o}\rangle (\varepsilon_j - \varepsilon_\nu) \right] c_j$

Exact MTO theory (1994):

Give the partial wave, $\phi_{RL}(\epsilon, r_R)$, a tail, which sticks into the interstitial:

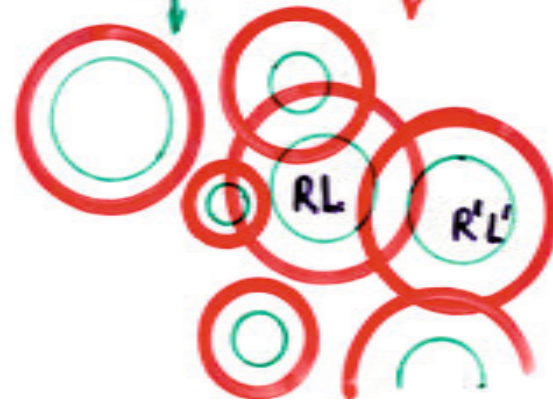
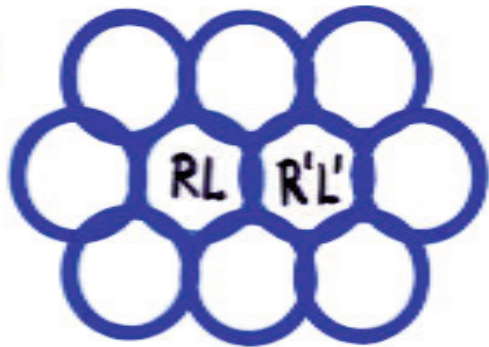
Before: 1. & 2. gen.



Now: 3. gen.



ASA:



4.1 EMTOs

In this section we define the set of exact, energy-dependent MTOs (EMTOs) and use them to derive the screened KKR equations and canonical band theory. We first explain what the EMTOs are, starting with their envelope functions, and only thereafter, how to construct them.

Since EMTOs use *overlapping* MT-potentials, can form *truly* minimal sets, and are usually *localized*, their definition is tricky:

The members, $h_{\bar{R}\bar{l}\bar{m}}^\alpha(\varepsilon, \mathbf{r}_R)$, of the set of *envelopes*, $|h^\alpha(\varepsilon)\rangle$, are superpositions of *bare* spherical waves, $h_{Rlm}(\varepsilon, \mathbf{r}_R)$, all with the same energy $\kappa^2 = \varepsilon$, and are called *screened spherical waves*:

$$|h^\alpha(\varepsilon)\rangle = |h(\varepsilon)\rangle M^\alpha(\varepsilon).$$

Such a set is characterized, first of all, by the set of Rlm -values to be included in the set, the so-called *active* Rlm -values. Secondly, by a set of non-overlapping *hard-spheres* with radii a_R . And, thirdly, for the *passive* Rlm -values, by the *phase shifts* $\eta_{Rl}(\varepsilon)$ of the model potential. With such a division into active and passive channels, a choice of hard spheres for the former, and the phase shifts for the latter, we can state the boundary condition to be satisfied for a member,

$h_{\bar{R}\bar{l}\bar{m}}^\alpha(\varepsilon, \mathbf{r}_R)$, of the set: Its spherical-harmonics projections onto the hard spheres,

$$\mathcal{P}_{Rlm}^a \equiv \int d^3r \delta(a_R - r_R) Y_{lm}^*(\hat{\mathbf{r}}_R)$$

must *vanish* for all active Rlm -values, except for the own value, $\bar{R}\bar{l}\bar{m}$, for which we choose to normalize the hard-sphere projection to 1. For the remaining, passive Rlm values, $\mathcal{P}_{Rlm}^r h_{\bar{R}\bar{l}\bar{m}}^\alpha(\varepsilon, \mathbf{r}_{\bar{R}})$ should be a spherical wave, phase shifted by $\eta_{Rl}(\varepsilon)$. This holds automatically once l is so large ($> l_{max}=2-3$) that the phase shifts vanish.

With this boundary condition satisfied, the passive channels can be *augmented smoothly* with the appropriate Schrödinger solutions, $\varphi_{Rl}(\varepsilon, r_R)$, and the active channels, which usually diverge at the origin of r_R , can be *truncated* inside the hard spheres, i.e. for $r_R < a_R$. This truncation of the active channels is continuous for $Rlm \neq \bar{R}\bar{l}\bar{m}$, but jumps by 1 in the own channel. In all active channels there is a discontinuity of outwards *slope*,

$$\left. \frac{\partial}{\partial r} \mathcal{P}_{Rlm}^r h_{\bar{R}\bar{l}\bar{m}}^a(\varepsilon, \mathbf{r}_{\bar{R}}) \right|_{a_R} \equiv S_{Rlm, \bar{R}\bar{l}\bar{m}}^a(\varepsilon),$$

(for the own channel, the derivative should be taken slightly *outside* the sphere), specified by a *slope matrix*, which can be calculated as shown in the next section. The resulting augmented, truncated, and renor-

renormalized screened spherical wave, $\tilde{h}_{\bar{R}\bar{l}\bar{m}}^a(\varepsilon, \mathbf{r}_{\bar{R}}) \equiv \psi_{\bar{R}\bar{l}\bar{m}}^a(\varepsilon, \mathbf{r}_{\bar{R}})$, is now ready to have the hole in its own channel (head) filled:

The radial filling function is obtained by integrating the radial Schrödinger equation outwards from 0 to $s_{\bar{R}}$ with the proper potential, and from there, smoothly inwards to $a_{\bar{R}}$ with the flat (zero) potential. The solution, $\bar{\varphi}_{\bar{R}\bar{l}}(\varepsilon, r)$, for the flat potential, and of course the one, $\varphi_{\bar{R}\bar{l}}(\varepsilon, r)$, for the proper potential, are subsequently normalized such that the value of the former is 1 at $a_{\bar{R}}$. This is indicated by a superscript a :

$$\begin{aligned}\bar{\varphi}_{\bar{R}\bar{l}}^a(\varepsilon, r) &\equiv \bar{\varphi}_{\bar{R}\bar{l}}(\varepsilon, r) / \bar{\varphi}_{\bar{R}\bar{l}}(\varepsilon, a_{\bar{R}}), \\ \varphi_{\bar{R}\bar{l}}^a(\varepsilon, r) &\equiv \varphi_{\bar{R}\bar{l}}(\varepsilon, r) / \bar{\varphi}_{\bar{R}\bar{l}}(\varepsilon, a_{\bar{R}}).\end{aligned}$$

Finally, $\bar{\varphi}_{\bar{R}\bar{l}}^a(\varepsilon, r)$ is matched continuously, but with a kink to $\tilde{h}_{\bar{R}\bar{l}\bar{m}}^a(\varepsilon, \mathbf{r}_{\bar{R}})$, and it is truncated outside the interval $a_{\bar{R}} \leq r \leq s_{\bar{R}}$. The Schrödinger solution, $\varphi_{\bar{R}\bar{l}}(\varepsilon, r)$, is truncated outside the interval $0 \leq r \leq s_{\bar{R}}$. Hence, the resulting orbital has been constructed like an *accordion*: It starts from the origin as the regular Schrödinger solution which extends all the way out to the own potential sphere. Here, it is matched smoothly to a phase-shifted wave, which then runs inwards to the own hard sphere where it matches the screened spherical wave with a kink. Finally, the screened spherical wave continues outwards.

The active channels of the screened spherical wave are truncated inside all hard spheres with kinks, and the passive channels are substituted smoothly inside all hard spheres with regular Schrödinger solutions.

The EMTO, also called the *kinked partial wave*, is:

$$\begin{aligned}\phi_{\bar{R}\bar{l}\bar{m}}^a(\varepsilon, r_{\bar{R}}) &= [\varphi_{\bar{R}\bar{l}}^a(\varepsilon, r_{\bar{R}}) - \bar{\varphi}_{\bar{R}\bar{l}}^a(\varepsilon, r_{\bar{R}})] Y_{\bar{l}\bar{m}}(\hat{\mathbf{r}}_{\bar{R}}) \\ &\quad + \tilde{h}_{\bar{R}\bar{l}\bar{m}}^a(\varepsilon, \mathbf{r}_{\bar{R}}).\end{aligned}$$

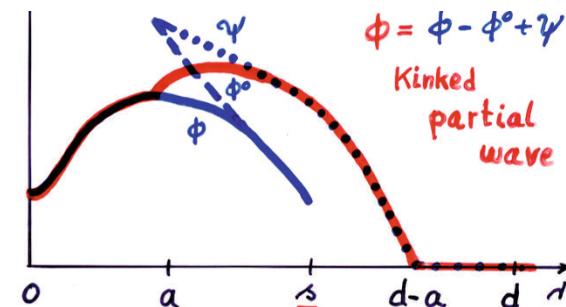
Here, the first term is the product of a spherical harmonic times a radial function, which vanishes smoothly at, and outside the own potential-sphere ($s_{\bar{R}}$). The second term is the augmented and truncated screened spherical wave, which matches onto the first, pure-angular-momentum term at the central hard sphere with a kink of size

$$S_{\bar{R}\bar{l}\bar{m}, \bar{R}\bar{l}\bar{m}}^a(\varepsilon) - \bar{\varphi}_{\bar{R}\bar{l}}^a(\varepsilon, a_{\bar{R}})',$$

where

$$' \equiv \partial/\partial r \quad \text{and} \quad \bar{\varphi}_{\bar{R}\bar{l}}^a(\varepsilon, a_{\bar{R}})' = D \{ \bar{\varphi}_{\bar{R}\bar{l}}(\varepsilon, a_{\bar{R}}) \} / a_{\bar{R}}.$$

Although the EMTO is everywhere continuous, it has kinks at the hard spheres in all active channels, but is smooth in the passive channels.



We can now try to make a *linear combination*,

$$\sum_{Rlm}^A \phi_{Rlm}^a(\varepsilon_i, r_R) c_{Rlm,i}^a,$$

of active (A) EMTOs which is *smooth*. This requires that its coefficients satisfy the *kink-cancellation condition*,

$$\sum_{\bar{R}\bar{l}\bar{m}}^A K_{Rlm, \bar{R}\bar{l}\bar{m}}^a(\varepsilon) c_{\bar{R}\bar{l}\bar{m}}^a = 0,$$

for each Rlm . Here we have multiplied each Rlm -equation by a_R^2 such that

$$K_{Rlm, \bar{R}\bar{l}\bar{m}}^a(\varepsilon) \equiv a_R^2 S_{Rlm, \bar{R}\bar{l}\bar{m}}^a(\varepsilon) - a_R D \{ \bar{\varphi}_{Rl}^a(\varepsilon, a_R) \} \delta_{R\bar{R}} \delta_{l\bar{l}} \delta_{m\bar{m}}.$$

becomes a *Hermitian* matrix. Since the passive channels are smooth by construction, the kink-cancellation condition must be solved only for the active channels and therefore constitute a set of homogeneous, linear equations. These have a proper solution for those energies, ε_i , which make the determinant of the matrix vanish. Most importantly, the corresponding linear combination is a *solution of Schrödinger's equation* at energy ε_i for the overlapping MT potential to 1st order in the overlap.

That this is true, can be seen from the following arguments: The kinks of an EMTO are always between two solutions of the same radial wave equation, either partial-wave projections of screened spherical waves, zero, or inwards integrated, phase-shifted waves. Since only two linearly independent radial solutions exist, e.g. Bessel and Neumann functions, it follows that, if they match without a kink at a_R , as they are required to do for the smooth linear combination of EMTOs, then they must be *identical in the entire range* $a_R \leq r \leq s_R$. This means that throughout the MT-sphere at \bar{R} ,

$$\begin{aligned} & \sum_{Rlm}^A \tilde{h}_{Rlm}^a(\varepsilon_i, \mathbf{r}_{\bar{R}}) c_{Rlm,i}^a \\ &= \sum_{\bar{l}\bar{m}}^A \bar{\varphi}_{\bar{R}\bar{l}}^a(\varepsilon_i, r_R) Y_{\bar{l}\bar{m}}(\hat{\mathbf{r}}_{\bar{R}}) c_{\bar{R}\bar{l}\bar{m},i}^a \\ & \quad + \sum_{\bar{l}\bar{m}}^P \varphi_{\bar{R}\bar{l}}^a(\varepsilon_i, r_R) Y_{\bar{l}\bar{m}}(\hat{\mathbf{r}}_{\bar{R}}) c_{\bar{R}\bar{l}\bar{m},i}^a. \end{aligned}$$

The last term comes from the passive (P) channels and the corresponding coefficients, $c_{P,i}^a$ are given by the solutions, $c_{A,i}^a$, of the kink-cancellation condition, times PA expansion coefficients. If site \bar{R} is passive (downfolded), only that term is present on the right-hand side. As a result, the smooth linear combination

reduces to:

$$\begin{aligned} & \sum_{Rlm}^A \phi_{Rlm}^a(\varepsilon_i, r_R) c_{Rlm,i}^a = \\ & \sum_{\bar{l}\bar{m}}^{A+P} \varphi_{\bar{R}\bar{l}}^a(\varepsilon_i, r_{\bar{R}}) Y_{\bar{l}\bar{m}}(\hat{\mathbf{r}}_{\bar{R}}) c_{\bar{R}\bar{l}\bar{m},i}^a + \quad (1) \\ & \sum_{R \neq \bar{R}}^A \sum_{lm}^A [\varphi_{Rl}^a(\varepsilon_i, r_R) - \bar{\varphi}_{Rl}^a(\varepsilon_i, r_R)] Y_{lm}(\hat{\mathbf{r}}_R) c_{Rlm,i}^a, \end{aligned}$$

near site \bar{R} . This is a solution of Schrödinger's equation, $\Psi_i(\varepsilon_i, \mathbf{r})$, plus an error consisting of *tongues* from the overlap of the neighboring muffin tins.

Now, the radial part of such a tongue is

$$\frac{1}{2} (s_R - r_R)^2 v_R(s_R) \varphi_{Rl}^a(\varepsilon, s_R),$$

to lowest order in $s_R - r_R$, as may be seen from the radial Schrödinger equation. Here, $v_R(s_R)$ is the MT-discontinuity. Operating finally with $\mathcal{H} - \varepsilon_i$ on the smooth linear combination of which (1) is the expansion

around site \bar{R} , yields the error:

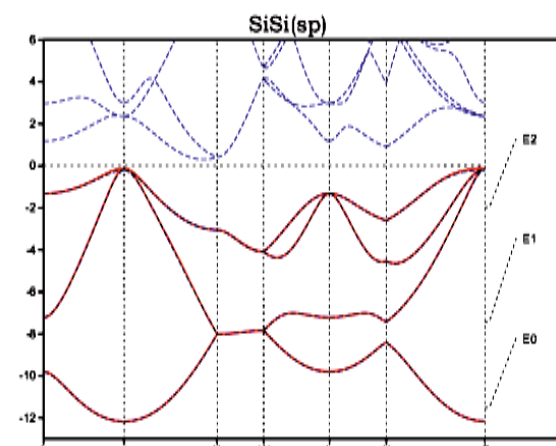
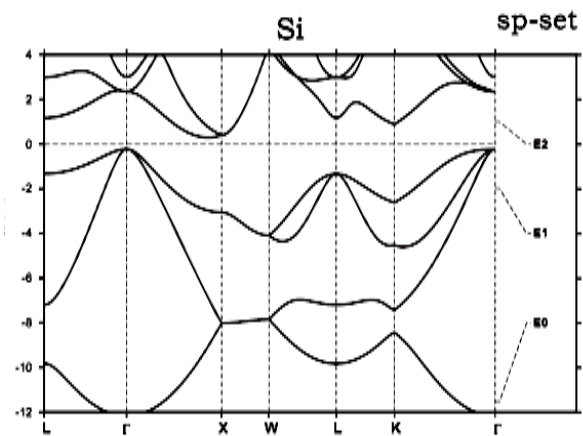
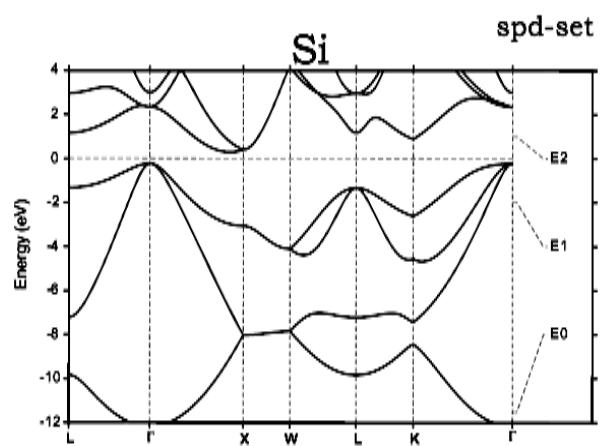
$$\begin{aligned} & \sum_{\bar{R}} v_{\bar{R}}(r_{\bar{R}}) \\ & \sum_{R \neq \bar{R}}^A \sum_{lm}^A [\varphi_{Rl}^a(\varepsilon_i, r_R) - \bar{\varphi}_{Rl}^a(\varepsilon_i, r_R)] Y_{lm}(\hat{\mathbf{r}}_R) c_{Rlm,i}^a \sim \\ & \frac{1}{2} \sum_{R\bar{R}}^{\text{pairs}} v_{\bar{R}}(r_{\bar{R}}) \left[(s_{\bar{R}} - r_{\bar{R}})^2 + (s_R - r_R)^2 \right] v_R(s_R) \Psi_i(\mathbf{r}), \end{aligned}$$

which is obviously of 2nd order in the potential overlap; Q.E.D.

The set of homogeneous linear equations:

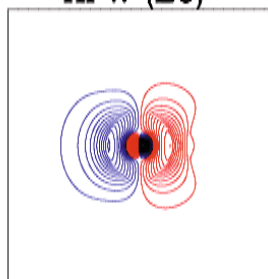
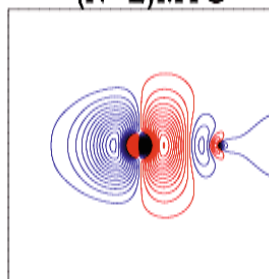
$$\sum_{\bar{R}\bar{l}\bar{m}}^A K_{Rlm, \bar{R}\bar{l}\bar{m}}^a(\varepsilon) c_{\bar{R}\bar{l}\bar{m}}^a = 0,$$

are the *screened KKR equations*, albeit in radial-derivative gauge (denoted by a latin superscript, e.g. a) rather than in phase-shift gauge (denote by the corresponding greek superscript, α).



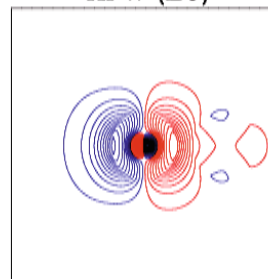
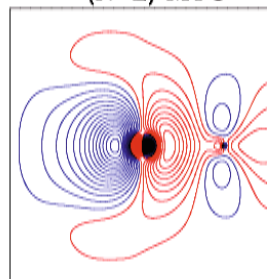
(N=2)MTO

KPW (E0)



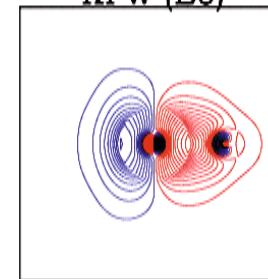
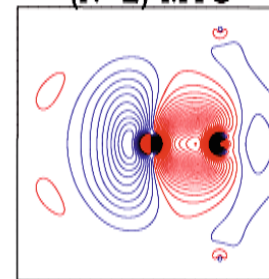
(N=2) MTO

KPW (E0)



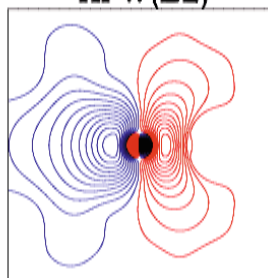
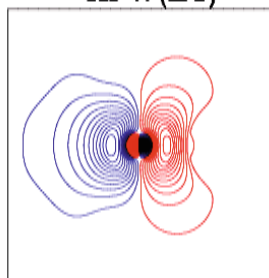
(N=2) MTO

KPW (E0)



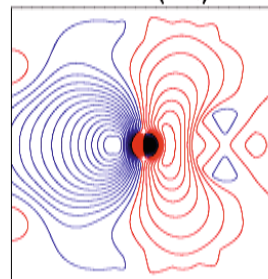
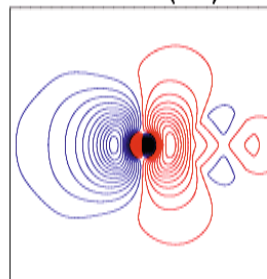
KPW(E1)

KPW(E2)



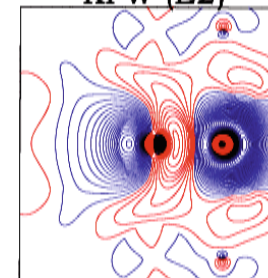
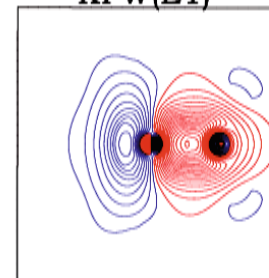
KPW (E1)

KPW (E2)

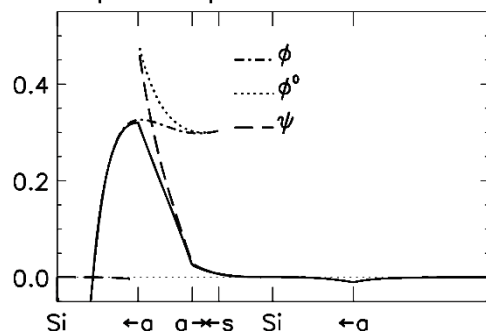


KPW(E1)

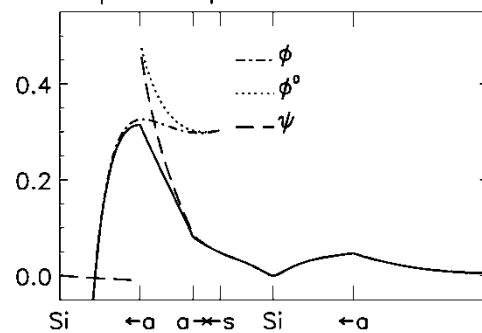
KPW (E2)



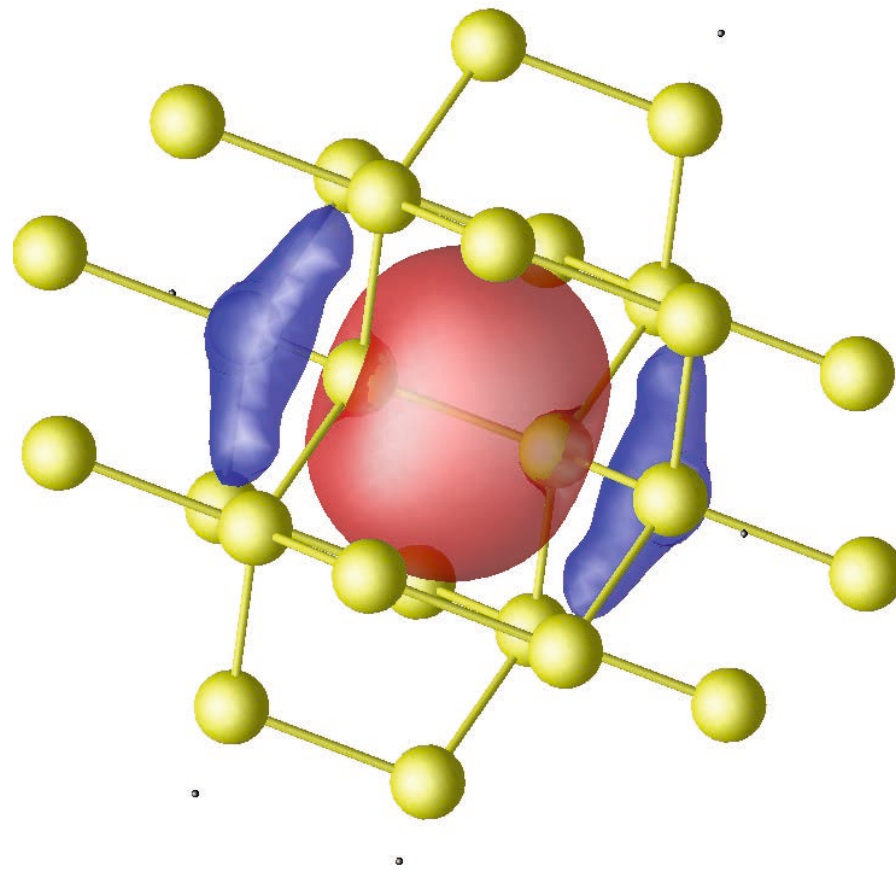
Si p kinked partial wave



Si p kinked partial wave



Si bond
orbital,
generated as
the sp^3 hybrid
formed from
the $SiSi(sp)$
NMTO
Wannier
Orbitals



4.1.1 Structure matrix

The bare Hankel function, $h_{Rlm}^0(\varepsilon, \mathbf{r}_R)$, to be used in the construction:

$$|h^\alpha(\varepsilon)\rangle = |h(\varepsilon)\rangle M^\alpha(\varepsilon),$$

of the envelopes, is a spherical harmonics times a radial function,

$$\begin{aligned} & \kappa^{l+1} [n_l(\kappa r) - ij_l(\kappa r)] \rightarrow \\ & -\frac{(2l-1)!!}{r^{l+1}} \left[1 + \frac{\varepsilon r^2}{2(2l-1)} \dots \right] \\ & -i\kappa \frac{(\varepsilon r)^l}{(2l+1)!!} \left[1 - \frac{\varepsilon r^2}{2(2l+3)} \dots \right], \end{aligned}$$

for $\varepsilon \rightarrow 0$. Here, $(2l+1)!! \equiv (2l+1)(2l-1)\dots 3 \cdot 1$ and $(-1)!! \equiv 1$. For $\varepsilon = \kappa^2 \leq 0$, this Hankel function is real and decays asymptotically as $e^{-r|\kappa|}/r$. The spherical Neumann and Bessel functions, normalized as respectively $\kappa^{l+1}n_l(\kappa r)$ and $\kappa^{-l}j_l(\kappa r)$, are real for all real energies and they are respectively irregular and regular at the origin. For $\varepsilon > 0$, the Hankel function therefore has an imaginary part, which is the solution for the homogeneous problem. The energy region of interest for the valence and low-lying conduction bands is $\varepsilon \sim 0$, and the advantage of using *screened* Hankel functions, $|h^\alpha(\varepsilon)\rangle = |h(\varepsilon)\rangle M^\alpha(\varepsilon)$,

is that in this region there are no solutions to the homogeneous hard-sphere problem; they start at higher energies. The screened Hankel functions are therefore localized and real.

In order to obtain explicit expressions for the transformation and slope matrices, $M^\alpha(\varepsilon)$ and $S^\alpha(\varepsilon)$, we first need to expand a bare spherical wave centered at \bar{R} in spherical harmonics around $R \neq \bar{R}$. Since the wave is regular around R , its expansion is in terms of Bessel functions and is:

$$\begin{aligned} n_{\bar{l}}(\kappa r_{\bar{R}}) Y_{\bar{l}\bar{m}}(\hat{\mathbf{r}}_{\bar{R}}) &= \sum_{lm} j_l(\kappa r_R) Y_{lm}(\hat{\mathbf{r}}_R) \sum_{l'} 4\pi \times \\ & i^{-\bar{l}+l-l'} C_{\bar{l}\bar{m},lm,l'} n_{l'}(\kappa |\bar{\mathbf{R}} - \mathbf{R}|) Y_{l' m - \bar{m}}^*(\widehat{\bar{\mathbf{R}} - \mathbf{R}}). \end{aligned}$$

Here, $n_{\bar{l}}$ and $n_{l'}$ can be any l -independent linear combination of a Neumann and a Bessel function. For a pure Bessel function, the expansion holds for all r_R , while for an irregular function, it holds for $r_R < |\bar{\mathbf{R}} - \mathbf{R}| \neq 0$. The l' -summation runs over

$$|l - \bar{l}|, |l - \bar{l}| + 2, \dots, l + \bar{l},$$

$i^{-\bar{l}+l-l'}$ is real, and

$$C_{\bar{l}\bar{m},lm,l'} \equiv \int Y_{\bar{l}\bar{m}}(\hat{r}) Y_{lm}^*(\hat{r}) Y_{l' m - \bar{m}}(\hat{r}) d\hat{r}.$$

Now, since we shall renormalize the Bessel and Neumann functions when changing to radial-derivative gauge, we can start out in phase-shift gauge and use these functions without prefactors which make them real, and for the Hankel function use: $\kappa [n_l(\kappa r) - i j_l(\kappa r)] \equiv h_l^0(\kappa r)$. The conventional bare structure matrix is then

$$B_{Rlm, \bar{R}\bar{l}\bar{m}}(\varepsilon) \equiv \sum_{l'} (-)^{\frac{-\bar{l}+l-l'}{2}} 4\pi \times \\ C_{\bar{l}\bar{m}, lm, l'}^{\kappa} h_{l'}^0(\kappa |\bar{\mathbf{R}} - \mathbf{R}|) Y_{l' m - \bar{m}}^* \left(\widehat{\bar{\mathbf{R}} - \mathbf{R}} \right)$$

and if we define the on-site part of the structure matrix as $B_{\bar{R}lm, \bar{R}\bar{l}\bar{m}}(\varepsilon) = -i\kappa \delta_{\bar{l}l} \delta_{\bar{m}m}$, the one-center expansions may be written as:

$$|h^0\rangle = |\kappa n\rangle + |j\rangle B. \quad (2)$$

Here and in the following $|\cdot\rangle$ is a row-vector of functions, B a matrix, and we have dropped the common energy argument.

This screening transformation, $|h^\alpha(\varepsilon)\rangle = |h(\varepsilon)\rangle M^\alpha(\varepsilon)$, is now defined by the requirement that the set of screened Hankel functions have one-center expansions formally similar to (2):

$$|h^\alpha\rangle = |h^0\rangle M^\alpha = |\kappa n\rangle + |j^\alpha\rangle B^\alpha, \quad (3)$$

but with modified radial tail-functions:

$$j_{Rlm}^\alpha(\varepsilon, r) \equiv j_l(\kappa r) - n_l(\kappa r) \tan \alpha_{Rlm}(\varepsilon). \quad (4)$$

Here, $\alpha_{Rlm}(\varepsilon)$ is the hard-sphere phase shift when Rlm is active and the proper phase shift when Rlm is passive, i.e.:

$$\tan \alpha_{Rlm}(\varepsilon) = \frac{j_l(\kappa a_R) D \{j_{Rlm}^\alpha(\varepsilon, a)\} - D \{j_l(\kappa a_R)\}}{n_l(\kappa a_R) D \{j_{Rlm}^\alpha(\varepsilon, a)\} - D \{n_l(\kappa a_R)\}}$$

with

$$D \{j_{Rlm}^\alpha(\varepsilon, a)\} \equiv \begin{cases} \infty & Rlm \in A \\ D \{\bar{\varphi}_{Rl}(\varepsilon, a_R)\} & Rlm \in P \end{cases}$$

$\alpha(\varepsilon)$ depends on m , only when the division into active and passive channels is m -dependent. This is the case, say, when one wants to select the Cu $d_{x^2-y^2}$ conduction band in a high-temperature superconducting cuprate. If we now insert Eq.s (4) and (2) in (3) and compare the coefficients of $|\kappa n\rangle$ and $|j\rangle$, we obtain the following expressions for the screening transformation and the screened structure matrix:

$$M^\alpha = \mathbf{1} - \frac{\tan \alpha}{\kappa} B^\alpha, \quad (5)$$

$$B^\alpha = \kappa \cot \alpha - \kappa \cot \alpha [B + \kappa \cot \alpha]^{-1} \kappa \cot \alpha$$

Here, all matrices are square with the high- l blocks neglected and $\kappa \cot \alpha$ is a diagonal matrix. We see that

the amount of lm -multipole charge at site R which screens the $\bar{l}\bar{m}$ -multipole at site \bar{R} , is

$$(\tan \alpha_{Rl}/\kappa) B_{Rlm, \bar{R}\bar{l}\bar{m}}^\alpha$$

By taking the radial derivatives at the hard spheres, we can find the desired expression for the slope matrix:

$$a^2 S^a(\varepsilon) = aD \{j(\kappa a)\} + \frac{1}{j(\kappa a)} [B(\varepsilon) + \kappa \cot \alpha(\varepsilon)]^{-1} \frac{1}{j(\kappa a)}.$$

Note that $\kappa \cot \alpha(\varepsilon)$ is real for all real energies and that

$$j(\kappa a) \kappa \cot \alpha(\varepsilon) j(\kappa a) \rightarrow \frac{1}{(2l+1)a} \frac{D \{j^\alpha(\varepsilon, a)\} + l + 1}{D \{j^\alpha(\varepsilon, a)\} - l}, \quad \text{for } \varepsilon \rightarrow 0.$$

For most purposes, the hard spheres can be taken to depend only on the type of atom, and it turns out that for respectively *spdf*-, *spd*-, *sp*-, and *s*-sets, the shortest range of the spherical waves is obtained for radial overlaps of $\omega_{R\bar{R}}^a = -15, -23, -36, \text{ and } -52\%$. In the first two cases, the range of the structure matrix is so short that it can be generated by inversion of $B(\varepsilon) + \kappa \cot \alpha(\varepsilon)$ in real space, using clusters of 20-50 sites. This is the basis of the *tight-binding* (TB) LMTO method to be derived below. Whereas a bare Hankel function has *pure* $\bar{l}\bar{m}$ character, and the bare structure matrix therefore transforms according to the Slater-Koster scheme, the screened structure matrix does *not*, because a screened Hankel function merely

has *dominant* $\bar{l}\bar{m}$ -character and tends to avoid the surrounding hard spheres.

Downfolding of channels with attractive potentials increases the range and energy dependence of the structure matrix $a^2 S^a(\varepsilon)$. Downfolding is therefore usually performed as a second, \mathbf{k} -space step, after the strongly screened structure matrix has been generated in real space and subsequently Bloch-summed to \mathbf{k} -space.

4.1.2 Canonical band theory

Screening provides short range and removes the violent energy dependence of the structure matrix which originates from the oscillatory behavior of the bare Hankel functions for positive energy. For closely packed structures and with strong screening, one may even approximate the energy dependence of the structure matrix by its 1st-order Taylor series around $\varepsilon=0$. For this, only the simple power-law expressions for the Bessel and Neumann functions given by:

$$\lim_{\varepsilon \rightarrow 0} \kappa^{l+1} [n_l(\kappa r) - i j_l(\kappa r)] = -\frac{(2l-1)!!}{r^{l+1}} \left[1 + \frac{\varepsilon r^2}{2(2l-1)} \dots \right] - i\kappa \frac{(\varepsilon r)^l}{(2l+1)!!} \left[1 - \frac{\varepsilon r^2}{2(2l+3)} \dots \right],$$

are needed. The kink-cancellation equations:

$$\sum_{\bar{R}\bar{l}\bar{m}}^A K_{Rlm, \bar{R}\bar{l}\bar{m}}^a(\varepsilon) c_{\bar{R}\bar{l}\bar{m}}^a = 0,$$

now offer an intelligible and general solution to the Wigner-Seitz problem (Sect. 2) in terms of radial logarithmic derivative functions, $D\{\bar{\varphi}(\varepsilon, a)\}$, characterizing the *potential* and matrices, $aS^a(0)$ and $a\dot{S}^a(0)$, specifying the boundary conditions set by the *structure*.

This canonical band theory originally relied on the *atomic spheres approximation* (ASA), but the current form includes both the so-called *combined-correction* term, expressed by $\dot{S}^a(0)$, and also allows for *down-folding*, to the extent that the approximation $S^a(\varepsilon) \approx S^a(0) + \varepsilon\dot{S}^a(0)$ holds. In order to come even closer to the original form in which the structure constants are completely independent of energy, we must neglect the off-diagonal elements of $a\dot{S}^a(0)$ and subtract the diagonal element from $D\{\bar{\varphi}(\varepsilon, a)\}$. The resulting diagonal element can finally be related to the logarithmic derivative, $D\{\bar{\varphi}_{Rl}(\varepsilon, q_{Rlm})\}$, evaluated at a "magic" radius q_{Rlm} , to be specified in Sect. ??.

With *original* normalizations, the screened KKR-ASA matrix is $P^\alpha(\varepsilon) - S^\alpha$, which is Hermitian. Here, the ever increasing *potential functions* are:

$$\begin{aligned} P^\alpha(\varepsilon) &= \frac{W\{n(r), \bar{\varphi}(\varepsilon, r)\}}{W\{j^\alpha(r), \bar{\varphi}(\varepsilon, r)\}} = \frac{P(\varepsilon)}{1 - \alpha P(\varepsilon)} \\ &= -2 \left(\frac{w}{a}\right)^{2l} [D\{\bar{\varphi}(\varepsilon, a)\} + l + 1], \end{aligned}$$

with

$$W\{f(r), g(r)\} \equiv r^2 [f(r)g(r)' - f(r)g(r)'],$$

being the Wronskian, which is independent of r , if f and g are solutions of the same radial Schrödinger equation. The original structure matrix is:

$$S^\alpha \equiv -2 \left(\frac{w}{a}\right)^l [S^a(0) + l + 1] \left(\frac{w}{a}\right)^{\bar{l}+1},$$

with $l + 1$ to be regarded as a diagonal matrix. With these normalizations, the screening relation:

$$B^\alpha = \kappa \cot \alpha - \kappa \cot \alpha [B + \kappa \cot \alpha]^{-1} \kappa \cot \alpha$$

becomes:

$$S^\alpha = \alpha^{-1} (\alpha^{-1} - S)^{-1} \alpha^{-1} - \alpha^{-1},$$

with screening constants:

$$\alpha \equiv (a/w)^{2l+1} / [2(2l+1)].$$

The *bare* structure matrix is given by:

$$S_{ll'm} = (-)^{l'+m+1} 2 (l+l')! \times \left[\frac{(2l+1)(2l'+1)}{(l+m)!(l-m)!(l'+m)!(l'-m)!} \right]^{\frac{1}{2}} \left(\frac{w}{d} \right)^{l+l'+1}$$

when the z -axis is turned from the first to the second orbital, and d is the distance. This simple expression yields bare *canonical hopping integrals* such as

$$S_{dd(\sigma,\pi,\delta)} = (-6, 4, -1) 10 (w/d)^5,$$

which are useful for rough estimates, in particular for p , d , and f orbitals. To turn the z -axis in an arbitrary direction, the Slater-Koster scheme may be used. For the hopping integrals involving d orbitals, the canonical values were used in W.A. Harrison's Periodic Table, which however for the s and p orbitals used free-electron-like scaling, $S \propto d^{-2}$.

The KKR-ASA matrix has been used to explain the band structures of close packed, elemental crystals in terms of *potential parameters* and *canonical l -bands*: The band positions, C_l , widths, Δ_l , and shapes, γ_l , parametrize the bare potential function,

$$P^\alpha(\varepsilon) = \frac{P(\varepsilon)}{1 - \alpha P(\varepsilon)} = -2 \left(\frac{w}{a} \right)^{2l} [D\{\bar{\varphi}(\varepsilon, a)\} + l + 1]$$

as

$$\frac{1}{P_{Rl}^\alpha(\varepsilon)} + \alpha_l = \frac{1}{P_{Rl}(\varepsilon)} = \frac{\Delta_{Rl}}{\varepsilon - C_{Rl}} + \gamma_{Rl} + \dots,$$

and the *canonical l -bands*, $S_{li}^{\alpha k}$, are the $m\bar{m}$ -diagonalized

ll -blocks of the screened structure matrix in k -space. In terms of these quantities, the *unhybridized l -bands* are:

$$\varepsilon_{li}^k = C_{Rl} + \Delta_{Rl} \frac{S_{li}^{\alpha k}}{1 - (\gamma_{Rl} - \alpha_l) S_{li}^{\alpha k}}.$$

The KKR equations of course include hybridization, and with the screening constants chosen to be the band-shape parameters γ_{Rl} , the KKR-ASA matrix, $P^\gamma(\varepsilon) - S^\gamma$, takes the form of a 2-center Hamiltonian:

$$H_{Rlm, \bar{R}\bar{l}\bar{m}}^\gamma = C_{Rl} \delta_{R\bar{R}} \delta_{l\bar{l}} \delta_{m\bar{m}} + \Delta_{Rl}^{1/2} S_{Rlm, \bar{R}\bar{l}\bar{m}}^{\gamma k} \Delta_{\bar{R}\bar{l}}^{1/2}.$$

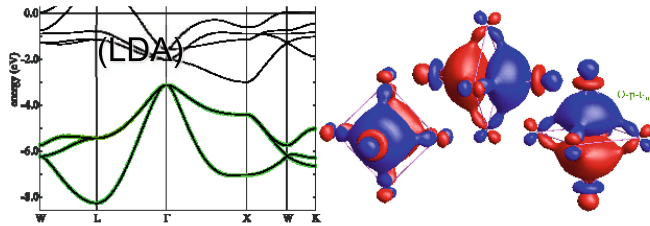
Its eigenvalues turn out to be the energies to 2nd order in their deviation from the energy, ε_ν , for which the potential parameters are calculated. This form is general and includes the hybridization between Rl bands in compounds. The form valid for arbitrary, potential independent screening is a Hamiltonian to 1st order, only. It is given by

$$H = \dot{P}^{\frac{1}{2}} E \dot{P}^{-\frac{1}{2}} = \varepsilon_\nu - (P/\dot{P}) + \dot{P}^{-\frac{1}{2}} S \dot{P}^{-\frac{1}{2}}.$$

Screened canonical band theory based on the approximate KKR matrix, $P^\alpha(\varepsilon) - S^\alpha$, has been very useful in combination with the coherent-potential approximation (CPA) for substitutionally disordered alloys, as well as in Green-function calculations for extended defects, such as surfaces and interfaces. Recently, the EMTO method was implemented for such calculations.

Multiplet ligand-field theory using Wannier orbitals

M. W. Haverkort,¹ M. Zwierzycki,² and O. K. Andersen¹

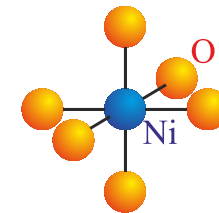


(LDA)

Different choices of Wannier-orbital sets:

5 Ni d WOs

Ni 3d⁸



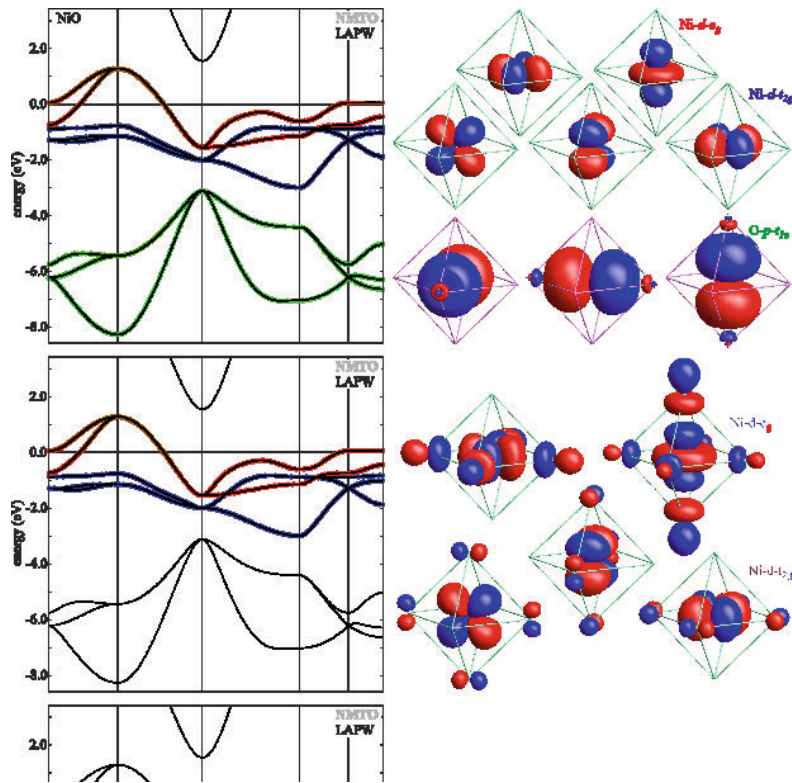
Simple electron count, but bad for the on-site-U approximation

3 O p WOs

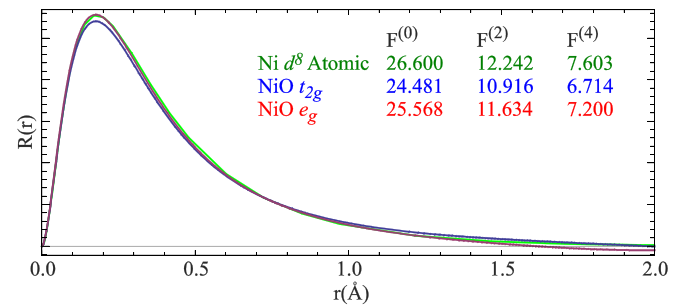
O 2p⁶

8 Ni d + O p WOs

O 2p^{5.4} Ni 3d^{8.6}



Almost atomic 3d orbitals,
 the on-site-U approximation is good,
 but the electron count is non-trivial



5.2 NMTOs

We now want to construct energy-*independent* orbitals. Specifically, we want to make a superposition of the set of EMTOs,

$$\phi_{\bar{R}\bar{l}\bar{m}}^a(\varepsilon, r_{\bar{R}}) = \left[\varphi_{\bar{R}\bar{l}}^a(\varepsilon, r_{\bar{R}}) - \bar{\varphi}_{\bar{R}\bar{l}}^a(\varepsilon, r_{\bar{R}}) \right] Y_{\bar{l}\bar{m}}(\hat{\mathbf{r}}_{\bar{R}}) + \tilde{h}_{\bar{R}\bar{l}\bar{m}}^a(\varepsilon, \mathbf{r}_{\bar{R}}),$$

evaluated at a mesh of energies, $\epsilon_0, \dots, \epsilon_N$, such that the resulting set of NMTOs,

$$\begin{aligned} |\chi^{(N)}\rangle &= \sum_{n=0}^N |\phi(\epsilon_n)\rangle L_n^{(N)} \\ &= |\phi(\epsilon_N)\rangle + \frac{\Delta |\phi\rangle}{\Delta [N-1, N]} (E^{(N)} - \epsilon_N) + \dots \\ &\dots + \frac{\Delta^N |\phi\rangle}{\Delta [0\dots N]} (E^{(1)} - \epsilon_1) \dots (E^{(N)} - \epsilon_N), \end{aligned}$$

spans the solutions of Schrödinger's equation for the model potential to within an error given by:

$$\Psi_i(\mathbf{r}) - \Psi_i(\varepsilon_i, \mathbf{r}) \propto (\varepsilon_i - \epsilon_0)(\varepsilon_i - \epsilon_1) \dots (\varepsilon_i - \epsilon_N).$$

This is discrete polynomial approximation for a Hilbert space and $L_n^{(N)}$ are Lagrangian *matrices*, whose sum is the unit matrix. For $N=0$, the NMTO set is the set of EMTOs evaluated at the energy $\epsilon_0 \equiv \epsilon_\nu$. The second, rearranged series is Newton interpolation in terms of descending, i.e. starting at mesh-point N , fi-

nite differences. Here, $(E^{(1)} - \epsilon_1), \dots, (E^{(N)} - \epsilon_N)$, is a product of energy *matrices*, which in general are not Hermitian and do not commute. The NMTO is independent of the order of the energy points, but the individual terms in the Newton series are not, and this series is only used with the energies ordered according to size, in which case it has a clear interpretation. If the energy mesh condenses onto ϵ_ν , then

$$\frac{\Delta^N \phi}{\Delta [0\dots N]} \rightarrow \frac{1}{N!} \left. \frac{d^N \phi}{d\varepsilon^N} \right|_{\epsilon_\nu},$$

and the Newton series becomes a truncated Taylor series. For the present purpose, where we want to be able to use up to about 5 energies, the Taylor series is not practical, in particular because evaluation of the NMTO Hamiltonian and overlap matrices will require taking energy derivatives of orders $2N$ and $2N + 1$ respectively. A useful, general expression for a divided difference is:

$$\frac{\Delta^N \phi}{\Delta [0\dots N]} = \sum_{n=0}^N \frac{\phi(\epsilon_n)}{\prod_{m=0, \neq n}^N (\epsilon_n - \epsilon_m)}.$$

We have dropped all superscripts a because, from now on, they do not change; screening and downfolding is done at the level of forming the EMTOs. Note that, in contrast to LMTO sets of the 2nd generation, NMTO sets for different screenings span different Hilbert spaces; the factor in front of $(\epsilon_i - \epsilon_0) \cdot (\epsilon_i - \epsilon_N)$ depends on a . It is obvious that for N given, the error must increase with the degree of downfolding, because downfolding decreases the size of the basis set. This, on the other hand, makes it necessary to go beyond linear basis sets if one wants to generate truly minimal basis sets, able to select merely the *occupied* bands of an insulator, or a few narrow d -bands of a transition-metal oxide.

Downfolding followed by construction of an NMTO basis set is very different from standard Löwdin downfolding, which partitions a *given*, large (say orthonormal) basis into active and passive subsets, then finds the downfolded Hamiltonian matrix as

$$\begin{aligned} \langle A(\epsilon) | \mathcal{H} | A(\epsilon) \rangle &= \langle A | \mathcal{H} | A \rangle \\ &- \langle A | \mathcal{H} | P \rangle \langle P | \mathcal{H} - \epsilon | P \rangle^{-1} \langle P | \mathcal{H} | A \rangle, \end{aligned}$$

and finally removes the ϵ -dependence of the downfolded basis by *linearizing* $\langle P | \mathcal{H} - \epsilon | P \rangle^{-1}$ and treating the term linear in ϵ as an overlap matrix. Obviously, an NMTO set with $N \geq 1$ is more accurate.

NMTOs can be used to generate Wannier functions directly, because with an appropriate choice of active channels, one can generate an NMTO set for the isolated set of bands in question. Upon making the mesh finer, the NMTO set will converge to the proper Hilbert space spanned by any set of Wannier functions. After orthonormalization, the NMTO set will therefore *be* a set of Wannier functions. NMTOs are localized *a priori* by virtue of the hard-sphere confinement of the constituent EMTOs, and since NMTOs are not orthonormal, they can –but must not– be more localized than maximally localized Wannier functions.

We shall now see that the Lagrangian matrices as well as the Hamiltonian and overlap matrices for the model potential, are all expressed solely in terms of the kink- or KKR matrix, $K_{Rlm, \bar{R}\bar{l}\bar{m}}^a(\epsilon)$, and its first energy derivative matrix evaluated at points of the energy mesh. In fact, the NMTO formalism is much simpler if expressed in terms of the Green matrix, $G(\epsilon) \equiv K(\epsilon)^{-1}$, also called the resolvent and, in multiple scattering theory, the scattering path operator.

Since a single EMTO, $\phi_{\bar{R}\bar{l}\bar{m}}^a(\epsilon, r_{\bar{R}})$, solves Schrödinger's differential equation for the model potential, except at the kinks, operation with the Hamiltonian gives a series of delta-functions at the hard spheres and for the

active channels:

$$(\varepsilon - \mathcal{H}) \phi_{\bar{R}\bar{l}\bar{m}}(\varepsilon, \mathbf{r}) = \sum_{Rlm}^A \delta(r_R - a_R) Y_{lm}(\hat{\mathbf{r}}_R) K_{Rlm, \bar{R}\bar{l}\bar{m}}(\varepsilon).$$

Solving for $\delta(r_R - a_R) Y_L(\hat{\mathbf{r}}_R)$, leads to:

$$\delta(r_R - a_R) Y_L(\hat{\mathbf{r}}_R) = (\varepsilon - \mathcal{H}) \sum_{\bar{R}\bar{l}\bar{m}}^A \phi_{\bar{R}\bar{l}\bar{m}}(\varepsilon, \mathbf{r}) G_{\bar{R}\bar{l}\bar{m}, Rlm}(\varepsilon)$$

which shows that the linear combinations,

$$\gamma_{Rlm}(\varepsilon, \mathbf{r}) = \sum_{\bar{R}\bar{l}\bar{m}}^A \phi_{\bar{R}\bar{l}\bar{m}}(\varepsilon, \mathbf{r}) G_{\bar{R}\bar{l}\bar{m}, Rlm}(\varepsilon),$$

of EMTOs –all with the same energy and screening– may be considered a Green function, $G(\varepsilon, \bar{\mathbf{r}}, \mathbf{r})$, which has $\bar{\mathbf{r}}$ *confined* to the hard spheres, i.e. $\bar{\mathbf{r}} \rightarrow Rlm$. Considered a function of \mathbf{r} , this Green function is a solution with energy ε of the Schrödinger equation, except at its own sphere and for its own angular momentum, where it has a kink of size unity. This kink becomes negligible when ε is close to a one-electron energy, because the Green function has a pole there. The confined Green function is factorized into a vector of EMTOs, $|\phi(\varepsilon)\rangle$, which has the full spatial dependence and a weak energy dependence, and a Green matrix, $G(\varepsilon)$, which has the full energy dependence.

Now, we want to factorize the \mathbf{r} and ε -dependences *completely* and, hence, to approximate the confined Green function, $|\phi(\varepsilon)\rangle G(\varepsilon)$, by $|\chi^{(N)}\rangle G(\varepsilon)$:

Note that subtracting from the Green function a function which is analytical in energy and remains in the Hilbert space spanned by the set $|\phi(\varepsilon_n)\rangle$ produces an equally good Green function, in the sense that both yield the same solutions of Schrödinger's equation. We therefore first define a set $|\chi^{(N)}(\varepsilon)\rangle$ by:

$$|\gamma(\varepsilon)\rangle = |\phi(\varepsilon)\rangle G(\varepsilon) \equiv |\chi^{(N)}(\varepsilon)\rangle G(\varepsilon) + \sum_{n=0}^N |\phi(\varepsilon_n)\rangle G(\varepsilon_n) A_n^{(N)}(\varepsilon),$$

and then determine the analytical functions, $A_n^{(N)}(\varepsilon)$, in such a way that $|\chi^{(N)}(\varepsilon)\rangle$ takes the *same* value, $|\chi^{(N)}\rangle$, at all mesh points. If that can be done,

$$|\chi^{(N)}(\varepsilon)\rangle = |\chi^{(N)}\rangle + O((\varepsilon - \varepsilon_0) \dots (\varepsilon - \varepsilon_N)),$$

and $|\chi^{(N)}\rangle$ is the set of NMTOs. Now, since

$$|\chi^{(N)}(\varepsilon_0)\rangle = \dots = \chi^{(N)}(\varepsilon_N),$$

the N th divided difference of $|\chi^{(N)}(\varepsilon)\rangle G(\varepsilon)$ equals $|\chi^{(N)}\rangle$ times the N th divided difference of $G(\varepsilon)$.

Moreover, if we let $A_n^{(N)}(\varepsilon)$ be a polynomial of $(N-1)$ st degree (N th degree yields zero-solutions for the NMTOs), their N th divided difference on the mesh will vanish. As a result

$$\left| \frac{\Delta^N \gamma}{\Delta [0\dots N]} \right\rangle = \frac{\Delta^N}{\Delta [0\dots N]} |\phi\rangle G = |\chi^{(N)}\rangle \frac{\Delta^N G}{\Delta [0\dots N]},$$

and we have therefore found the solution:

$$|\chi^{(N)}\rangle = \frac{\Delta^N |\phi\rangle G}{\Delta [0\dots N]} \left(\frac{\Delta^N G}{\Delta [0\dots N]} \right)^{-1}$$

for the NMTO set. The divided difference of the product is easily evaluated:

$$\frac{\Delta^N |\phi\rangle G}{\Delta [0\dots N]} = \sum_{n=0}^N \frac{|\phi(\varepsilon_n)\rangle G(\varepsilon_n)}{\prod_{m=0, \neq n}^N (\varepsilon_n - \varepsilon_m)},$$

in terms of the values of the EMTOs and the Green matrix on the energy mesh. This expression, together with the similar one for $\Delta^N G / \Delta [0\dots N]$, are those needed to determine the Lagrange matrices in:

$$\begin{aligned} |\chi^{(N)}\rangle &= \sum_{n=0}^N |\phi(\varepsilon_n)\rangle L_n^{(N)} = \\ &|\phi(\varepsilon_N)\rangle + \frac{\Delta |\phi\rangle}{\Delta [N-1, N]} (E^{(N)} - \varepsilon_N) + \dots \\ &\dots + \frac{\Delta^N |\phi\rangle}{\Delta [0\dots N]} (E^{(1)} - \varepsilon_1) \dots (E^{(N)} - \varepsilon_N). \end{aligned}$$

For $N = 0$, the NMTO set is of course the set of EMTOs evaluated at ε_0 :

$$|\chi^{(0)}\rangle = |\phi(\varepsilon_0)\rangle.$$

NMTOs with $N > 0$ are *smooth*, because according to:

$$\begin{aligned} \delta(r_R - a_R) Y_L(\hat{\mathbf{r}}_R) = \\ (\varepsilon - \mathcal{H}) \sum_{\bar{R}\bar{l}\bar{m}}^A \phi_{\bar{R}\bar{l}\bar{m}}(\varepsilon, \mathbf{r}) G_{\bar{R}\bar{l}\bar{m}, Rlm}(\varepsilon), \end{aligned}$$

the kinks of $|\gamma(\varepsilon)\rangle$ are independent of ε . This does however not imply that for a single NMTO, the EMTO accordion is completely compressed, like for a smooth linear combination of EMTOs,

$$\sum_{Rlm \in A} \phi_{Rlm}^a(\varepsilon_i, r_R) c_{Rlm,i}^a,$$

with the same energy. The linear combinations making up an NMTO have *different* energies and, as a consequence, discontinuities remain in $(2N+1)$ st radial derivatives at the hard spheres. Projecting an NMTO onto an active channel, leads to a radial function of the type $\varphi(r) - \bar{\varphi}(r) + \mathcal{P}^r \tilde{h}(\mathbf{r})$, where $\varphi(r) - \bar{\varphi}(r) \propto (s-r)^2$ near s , and where near a ,

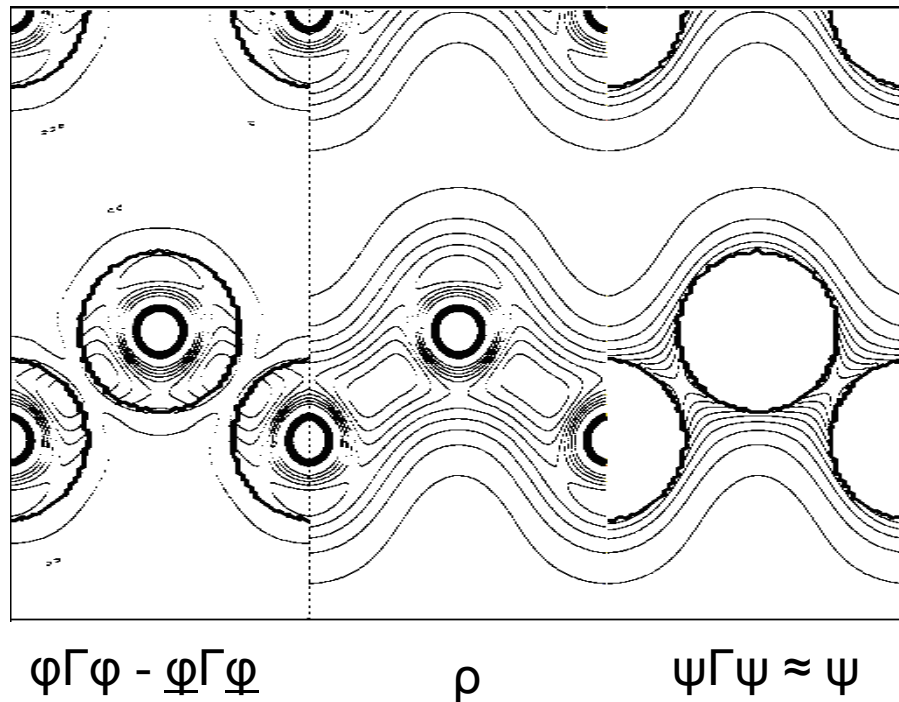
$$\mathcal{P}^r \tilde{h}(\mathbf{r}) - \bar{\varphi}(r) \propto (r-a)^{2N+1} (\varepsilon - \varepsilon_0) \dots (\varepsilon - \varepsilon_N).$$

Since the latter error is of the same order as $\Psi_i(\mathbf{r}) - \Psi_i(\epsilon_i, \mathbf{r}) \propto (\epsilon_i - \epsilon_0)(\epsilon_i - \epsilon_1) \dots (\epsilon_i - \epsilon_N)$, it should be included there. This means that cross-terms between φ , $\bar{\varphi}$, and $\mathcal{P}^r \tilde{h}$ can be neglected, and that leads to the following simple prescription for evaluating the product of two EMTOs with different energies:

$$|\phi\rangle\langle\phi| = |\varphi Y\rangle\langle Y\varphi| - |\bar{\varphi} Y\rangle\langle Y\bar{\varphi}| + |\tilde{h}\rangle\langle\tilde{h}|, \quad (6)$$

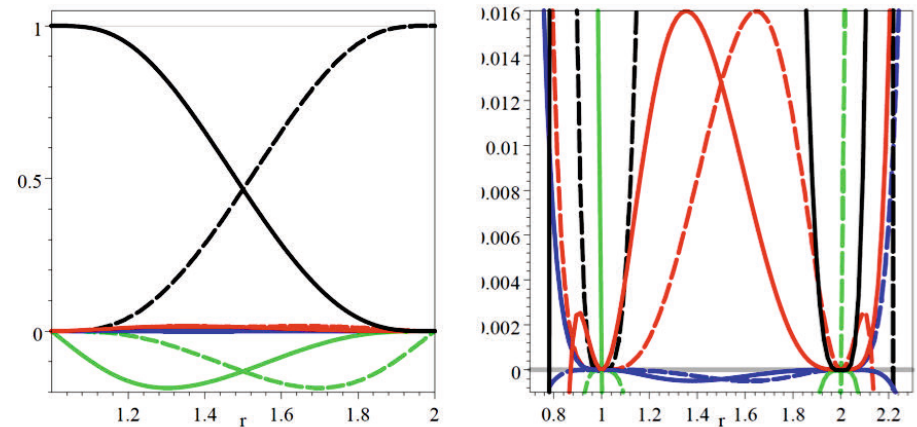
occurring in the expression for $|\chi^{(N)}\rangle\langle\chi^{(N)}|$, which is needed for evaluation of matrix elements and the charge density.

Si charge density



The sum of the first two terms in (6) is simply a finite sum of spherical harmonics times radial functions which vanish smoothly outside the MT spheres. The third term is more complicated because the SSWs do not have pure lm -character but merely short range. What we know about the SSWs is the structure matrix which specifies the spherical-harmonics expansions of the radial derivatives at the hard spheres.

It is therefore practical to *interpolate* a *product* of *strongly* screened spherical waves across the hard-sphere interstitial by a *sum* of SSWs. Specifically, we fit—at all spheres and for all spherical-harmonics with $l \lesssim 6$ —the radial values plus first 3 derivatives of the product (e.g. the charge-density) to those of a sum of SSWs with 4 different energies. The so-called *value-and-derivative functions*, each one vanishing in all channels except its own, are purely structural and exceedingly well localized because the value and first 3 derivatives vanish at all *other* spheres.



With this representation of the charge density Poisson's equation is solved analytically. We now have an efficient self-consistent, full-potential NMTO code employing this technique [Y. Nohara and OKA].

In order to figure out how the Hamiltonian operates on an NMTO, we use:

$$(\varepsilon - \mathcal{H}) \phi_{\bar{R}\bar{l}\bar{m}}(\varepsilon, \mathbf{r}) = \sum_{Rlm}^A \delta(r_R - a_R) Y_{lm}(\hat{\mathbf{r}}_R) K_{Rlm, \bar{R}\bar{l}\bar{m}}(\varepsilon)$$

for $N=0$ and obtain: $\mathcal{H}|\chi^{(0)}\rangle = -|\delta\rangle K(\epsilon_0)$. For the smooth NMTOs with $N>0$ we can neglect the kink terms when operating on

$$|\phi(\varepsilon)\rangle G(\varepsilon) \equiv |\chi^{(N)}(\varepsilon)\rangle G(\varepsilon) + \sum_{n=0}^N |\phi(\epsilon_n)\rangle G(\epsilon_n) A_n^{(N)}(\varepsilon)$$

and then take the N th divided difference to get rid of the polynomials:

$$\begin{aligned} \mathcal{H} \left| \frac{\Delta^N \gamma}{\Delta[0\dots N]} \right\rangle &= \frac{\Delta^N}{\Delta[0\dots N]} |\varepsilon\gamma(\varepsilon)\rangle \\ &= \left| \frac{\Delta^{N-1} \gamma}{\Delta[0\dots N-1]} \right\rangle + \epsilon_N \left| \frac{\Delta^N \gamma}{\Delta[0\dots N]} \right\rangle. \end{aligned}$$

Solving for the NMTOs gives:

$$(\mathcal{H} - \epsilon_N) |\chi^{(N)}\rangle = |\chi^{(N-1)}\rangle (E^{(N)} - \epsilon_N),$$

with matrices, which are those entering the Newton series in:

$$\begin{aligned} |\chi^{(N)}\rangle &= \sum_{n=0}^N |\phi(\epsilon_n)\rangle L_n^{(N)} = \\ &|\phi(\epsilon_N)\rangle + \frac{\Delta|\phi\rangle}{\Delta[N-1, N]} (E^{(N)} - \epsilon_N) + \dots \\ &\dots + \frac{\Delta^N|\phi\rangle}{\Delta[0\dots N]} (E^{(1)} - \epsilon_1) \dots (E^{(N)} - \epsilon_N), \end{aligned}$$

given by:

$$E^{(M)} = \frac{\Delta^M \varepsilon G}{\Delta[0\dots M]} \left(\frac{\Delta^M G}{\Delta[0\dots M]} \right)^{-1}.$$

Expression $(\mathcal{H} - \epsilon_N) |\chi^{(N)}\rangle = |\chi^{(N-1)}\rangle (E^{(N)} - \epsilon_N)$ shows that increasing N increases the smoothness of the NMTOs and also their range, unless $E^{(N)}$ converges as is the case for a set of isolated bands. If $E^{(N)}$ is converged, so is the NMTO basis, and so is the Newton series. This series expresses the NMTO as a kinked partial wave at the same site and with the same angular momentum, plus a smoothing cloud of energy-derivative functions centered at all sites and with all angular momenta.

With the aim of obtaining the expressions for the overlap and Hamiltonian matrices needed in a variational calculation: $\sum_g (\langle \chi_{\bar{g}} | \mathcal{H} | \chi_g \rangle - \varepsilon \langle \chi_{\bar{g}} | \chi_g \rangle) b_g = 0$, we first find expressions involving $|\phi(\varepsilon)\rangle$ and $|\gamma(\varepsilon)\rangle$. Multiplication of

$$(\varepsilon - \mathcal{H}) \phi_{\bar{R}\bar{l}\bar{m}}(\varepsilon, \mathbf{r}) = \sum_{Rlm}^A \delta(r_R - a_R) Y_{lm}(\hat{\mathbf{r}}_R) K_{Rlm, \bar{R}\bar{l}\bar{m}}(\varepsilon).$$

from the left by $\langle \phi(\varepsilon) |$ and using:

$$|\phi\rangle \langle \phi| = |\varphi Y\rangle \langle Y \varphi| - |\bar{\varphi} Y\rangle \langle Y \bar{\varphi}| + |\tilde{h}\rangle \langle \tilde{h}|,$$

together with the facts that $\bar{\varphi}(\varepsilon, a) = 1$, that $\mathcal{P}^a \tilde{h}(\varepsilon, \mathbf{r}) = 1$ in the own channel, 0 in the other active channels, and solves the radial Schrödinger equation in the passive channels, leads to the result:

$$\langle \phi(\varepsilon) | \varepsilon - \mathcal{H} | \phi(\varepsilon) \rangle = K(\varepsilon). \quad (6)$$

Here again we have resorted to matrix notation. The Hamiltonian matrix for the $N=0$ set is thus

$$\langle \chi^{(0)} | \mathcal{H} - \varepsilon_0 | \chi^{(0)} \rangle = -K(\varepsilon_0).$$

In a similar way, and with the use of Green's second theorem, one finds that the overlap matrix between two EMTOs with different energies is:

$$\langle \phi(\bar{\varepsilon}) | \phi(\varepsilon) \rangle = \frac{K(\bar{\varepsilon}) - K(\varepsilon)}{\bar{\varepsilon} - \varepsilon} \quad (7)$$

$$\rightarrow \dot{K}(\varepsilon), \quad \text{for } \bar{\varepsilon} \rightarrow \varepsilon.$$

Note that by virtue of the definition of $|\tilde{h}\rangle$, there are no 3-center terms here. Hence, the overlap matrix for the $N=0$ set is simply:

$$\langle \chi^{(0)} | \chi^{(0)} \rangle = \langle \phi(\varepsilon_0) | \phi(\varepsilon_0) \rangle = \dot{K}(\varepsilon_0). \quad (8)$$

From Eq.s (6), (7), and:

$$\gamma_{Rlm}(\varepsilon, \mathbf{r}) = \sum_{\bar{R}\bar{l}\bar{m}}^A \phi_{\bar{R}\bar{l}\bar{m}}(\varepsilon, \mathbf{r}) G_{\bar{R}\bar{l}\bar{m}, Rlm}(\varepsilon),$$

one finds:

$$\begin{aligned} \langle \gamma(\bar{\varepsilon}) | \gamma(\varepsilon) \rangle &= -\frac{G(\bar{\varepsilon}) - G(\varepsilon)}{\bar{\varepsilon} - \varepsilon} \\ &\rightarrow \dot{G}(\varepsilon) = G(\varepsilon) \dot{K}(\varepsilon) G(\varepsilon), \quad \text{for } \bar{\varepsilon} \rightarrow \varepsilon. \end{aligned}$$

If we now take the M th divided difference with respect to $\bar{\varepsilon}$ and the N th with respect to ε , both on the mesh, then use $\frac{\Delta^N \phi}{\Delta[0\dots N]} = \sum_{n=0}^N \phi(\varepsilon_n) / \prod_{m=0, \neq n}^N (\varepsilon_n - \varepsilon_m)$ and order such that $M \leq N$, we find a double sum. If reordered to a single sum, with due care taken for the terms where $\bar{\varepsilon} = \varepsilon$, it reduces to the expression

$$\left\langle \frac{\Delta^M \gamma}{\Delta[0\dots M]} \middle| \frac{\Delta^N \gamma}{\Delta[0\dots N]} \right\rangle = -\frac{\Delta^{M+N+1} G}{\Delta[[0..M]..N]}, \quad (9)$$

where the right-hand side is minus the highest derivative of that polynomial of degree $M+N+1$ which coincides with $G(\varepsilon)$ at the points $\varepsilon_0, \dots, \varepsilon_N$ and has the same first derivatives $\dot{G}(\varepsilon)$ at the points $\varepsilon_0, \dots, \varepsilon_M$

(Hermit interpolation). For the matrix element of the Hamiltonian, expressions:

$$\mathcal{H} \left| \frac{\Delta^N \gamma}{\Delta [0..N]} \right\rangle = \left| \frac{\Delta^{N-1} \gamma}{\Delta [0..N-1]} \right\rangle + \epsilon_N \left| \frac{\Delta^N \gamma}{\Delta [0..N]} \right\rangle,$$

and (9) yield:

$$\begin{aligned} \left\langle \frac{\Delta^N \gamma}{\Delta [0..N]} \left| \mathcal{H} - \epsilon_N \right| \frac{\Delta^N \gamma}{\Delta [0..N]} \right\rangle &= \\ \left\langle \frac{\Delta^N \gamma}{\Delta [0..N]} \left| \frac{\Delta^{N-1} \gamma}{\Delta [0..N-1]} \right\rangle &= -\frac{\Delta^{2N} G}{\Delta [[0..N-1] N]}. \end{aligned}$$

The NMTO Hamiltonian and overlap matrices are thus given by the following, most elegant expression which involves nothing but the values and first derivatives of the KKR Green matrix, $G(\epsilon)$, on the energy mesh:

$$\begin{aligned} \frac{\Delta^N G}{\Delta [0..N]} \langle \chi^{(N)} | \mathcal{H} - \epsilon | \chi^{(N)} \rangle \frac{\Delta^N G}{\Delta [0..N]} \\ = \left(-\frac{\Delta^{2N} G}{\Delta [[0..N-1] N]} \right) - (\epsilon - \epsilon_N) \left(-\frac{\Delta^{2N+1} G}{\Delta [[0..N]]} \right). \end{aligned}$$

and with a simplified notation for the divided differences:

$$G [0..N] \langle \chi^{(N)} | \mathcal{H} - \epsilon | \chi^{(N)} \rangle G [0..N] = -G [[0..N-1] N] + (\epsilon - \epsilon_N) G [[0..N]]$$

Hence, the variational expression for the OMTA part of the Hamiltonian is:

$$\begin{aligned} \langle \chi^{(N)} | \mathcal{H} - \epsilon_N | \chi^{(N)} \rangle &= \\ -G [0..N]^{-1} G [[0..N-1] N] G [0..N]^{-1} \end{aligned}$$

and the overlap matrix is:

$$O^{(N)} \equiv \langle \chi^{(N)} | \chi^{(N)} \rangle = G [0..N]^{-1} G [[0..N]] G [0..N]^{-1}$$

The variational calculation will give eigenvalues, which for the model potential has errors proportional to $(\epsilon_i - \epsilon_0)^2 (\epsilon_i - \epsilon_1)^2 \dots (\epsilon_i - \epsilon_N)^2$.

In many cases one would like to work with a set of *orthonormal* NMTOs, e.g. *Wannier orbitals*, and preserve the *Rlm*-character of each NMTO. In order to arrive at this, we should – in the language of Löwdin – perform a *symmetrical orthonormalization* of the NMTO set. According to the expression for the overlap matrix, such a representation is obtained by the following transformation:

$$\begin{aligned} |\check{\chi}^{(N)}\rangle &= |\chi^{(N)}\rangle \{O^{(N)}\}^{-\frac{1}{2}} \\ &= |\chi^{(N)}\rangle G [0..N] \{-G [[0..N]]\}^{-\frac{1}{2}}, \end{aligned}$$

because it yields:

$$\begin{aligned} \langle \check{\chi}^{(N)} | \check{\chi}^{(N)} \rangle &= \\ -\{-G [[0..N]]\}^{-\frac{1}{2}\dagger} G [[0..N]] \{-G [[0..N]]\}^{-\frac{1}{2}} &= \mathbf{1} \end{aligned}$$

Note that this means:

$$-G [[0..N]] = \{-G [[0..N]]\}^{-\frac{1}{2}\dagger} \{-G [[0..N]]\}^{-\frac{1}{2}}.$$

In this orthonormal representation, the Hamiltonian matrix becomes:

$$\begin{aligned} & \langle \check{\chi}^{(N)} | \mathcal{H} - \epsilon_N | \check{\chi}^{(N)} \rangle = \\ & - \{ -G [[0..N]] \}^{-\frac{1}{2}\dagger} G [[0.N - 1] N] \{ -G [[0..N]] \}^{-\frac{1}{2}} \end{aligned}$$

To find an efficient way to *compute* the *square root* of the Hermitian, positive definite matrix $-G [[0..N]]$ may be a problem. Of course one may diagonalize the matrix, take the square root of the eigenvalues, and then back-transform, but this is time consuming. Cholesky decomposition is a better alternative, but that usually amounts to staying in the original representation. Löwdin orthogonalization works if the set is nearly orthogonal, because then the overlap matrix is nearly diagonal, and Löwdin's solution was to normalize the matrix such that it becomes 1 along the diagonal and then expand in the off-diagonal part, Δ :

$$(1 + \Delta)^{-\frac{1}{2}} = 1 - \frac{1}{2}\Delta + \frac{3}{8}\Delta^2 - \dots$$

This should work for the NMTO overlap matrix when the NMTOs are nearly orthogonal.

5.2.1 LMTOs

For $N=0$, we have the results:

$$\begin{aligned} | \chi^{(0)} \rangle &= | \phi(\epsilon_0) \rangle, \\ \langle \chi^{(0)} | \mathcal{H} - \epsilon_0 | \chi^{(0)} \rangle &= -K(\epsilon_0), \\ \langle \chi^{(0)} | \chi^{(0)} \rangle &= \langle \phi(\epsilon_0) | \phi(\epsilon_0) \rangle = \dot{K}(\epsilon_0). \end{aligned}$$

For comparison with conventional LMTOs, consider now the case $N=1$ with the two-point mesh condensed onto ϵ_ν , i.e., the tangent LMTO method. From

$$E^{(M)} = \frac{\Delta^M \epsilon G}{\Delta [0..M]} \left(\frac{\Delta^M G}{\Delta [0..M]} \right)^{-1}$$

we find the following energy matrix:

$$\begin{aligned} E^{(1)} &= \epsilon_\nu + G\dot{G}^{-1} = \epsilon_\nu - \dot{K}^{-1}K \\ &= \epsilon_\nu + \langle \phi | \phi \rangle^{-1} \langle \phi | \mathcal{H} - \epsilon_\nu | \phi \rangle, \end{aligned}$$

Here and in the following an omitted energy argument means that $\epsilon = \epsilon_\nu$. Insertion in the Taylor series yields:

$$| \chi^{(1)} \rangle = | \phi \rangle - | \dot{\phi} \rangle (E^{(1)} - \epsilon_\nu) = | \phi \rangle - | \dot{\phi} \rangle \dot{K}^{-1}K,$$

which shows that the LMTO is smooth and has the form anticipated in Sect. 1. The Hamiltonian and overlap matrices are:

$$\begin{aligned} \langle \chi^{(1)} | \mathcal{H} - \epsilon_\nu | \chi^{(1)} \rangle &= -\dot{G}^{-1} \frac{\ddot{G}}{2!} \dot{G}^{-1} = \\ &= -K + K\dot{K}^{-1} \frac{\ddot{K}}{2!} \dot{K}^{-1}K, \end{aligned}$$

$$\begin{aligned} \langle \chi^{(1)} | \chi^{(1)} \rangle &= -\dot{G}^{-1} \ddot{G} \dot{G}^{-1} = \\ &\dot{K} - K \dot{K}^{-1} \frac{\ddot{K}}{2!} - \frac{\ddot{K}}{2!} \dot{K}^{-1} K + K \dot{K}^{-1} \frac{\ddot{K}}{3!} \dot{K}^{-1} K. \end{aligned}$$

Had we instead used the Taylor series to compute the overlap matrix, we would of course have got the same result, and as consequences, $\ddot{K}=2! \langle \phi | \dot{\phi} \rangle$ and $\ddot{K}=3! \langle \dot{\phi} | \dot{\phi} \rangle$. This may also be obtained from the general relation:

$$\left\langle \frac{\Delta^M \gamma}{\Delta [0 \dots M]} \middle| \frac{\Delta^N \gamma}{\Delta [0 \dots N]} \right\rangle = -\frac{\Delta^{M+N+1} G}{\Delta [[0 \dots M] \dots N]}$$

Had we used the Taylor series to compute the Hamiltonian matrix, we would have used: $(\mathcal{H} - \epsilon_N) |\chi^{(N)}\rangle = |\chi^{(N-1)}\rangle (E^{(N)} - \epsilon_N)$ with $N=1$, to obtain the same result.

In order to make $E^{(1)}$ Hermitian and, hence, to transform it into a *1st-order Hamiltonian*:

$$H = \dot{K}^{\frac{1}{2}} E^{(1)} \dot{K}^{-\frac{1}{2}} = \epsilon_\nu - \dot{K}^{-\frac{1}{2}} K \dot{K}^{-\frac{1}{2}},$$

one must symmetrically orthonormalize the 0th-order set, which now becomes: $|\phi\rangle \langle \phi | \phi \rangle^{-\frac{1}{2}}$. After applying the same transformation to the LMTO set, it becomes:

$$|\chi^{(1)}\rangle = |\phi\rangle + |\dot{\phi}\rangle (H - \epsilon_\nu).$$

For simplicity of notation, we have not changed the symbols for the orbitals. This expression for the LMTO is the one envisaged in expression:

$$\begin{aligned} \varphi_{Rl}(\epsilon_\nu, r_R) + (\epsilon_i - \epsilon_\nu) \dot{\varphi}_{Rl}(\epsilon_\nu, r_R) = \\ \varphi_{Rl}(\epsilon_i, r_R) + O((\epsilon_i - \epsilon_\nu)^2). \end{aligned}$$

of Sect. 1: The tail-functions are $\dot{\phi}(\mathbf{r})$ and the head of the $\bar{R}\bar{l}\bar{m}$ -orbital is

$$\phi_{\bar{R}\bar{l}\bar{m}}(\mathbf{r}_{\bar{R}}) + \sum_{lm} \dot{\phi}_{\bar{R}lm}(\mathbf{r}_{\bar{R}}) (H - \epsilon_\nu)_{\bar{R}lm, \bar{R}\bar{l}\bar{m}}.$$

In order to show explicitly how the solutions of Schrödinger's equation for the solid can be described through overlap of orbitals, we may simply diagonalize H . Naming its eigenvectors and eigenvalues respectively $u_{Rlm,i}$ and ϵ_i , the linear combination of orbitals given by an eigenvector is:

$$\begin{aligned} |\hat{\chi}\rangle u_i &= |\phi\rangle u_i + |\dot{\phi}\rangle H u_i \\ &= [|\phi\rangle + |\dot{\phi}\rangle (\epsilon_i - \epsilon_\nu)] u_i \\ &= |\phi(\epsilon_i)\rangle u_i + O((\epsilon_i - \epsilon_\nu)^2), \end{aligned}$$

as anticipated. LMTOs thus naturally describe the way in which the overlap of orbitals leads to broadening of levels into bands.

Great simplification occurs if the energy dependence of the off-diagonal elements of the KKR matrix can be neglected, because then we can define,

$$K(\varepsilon) = P(\varepsilon) - S.$$

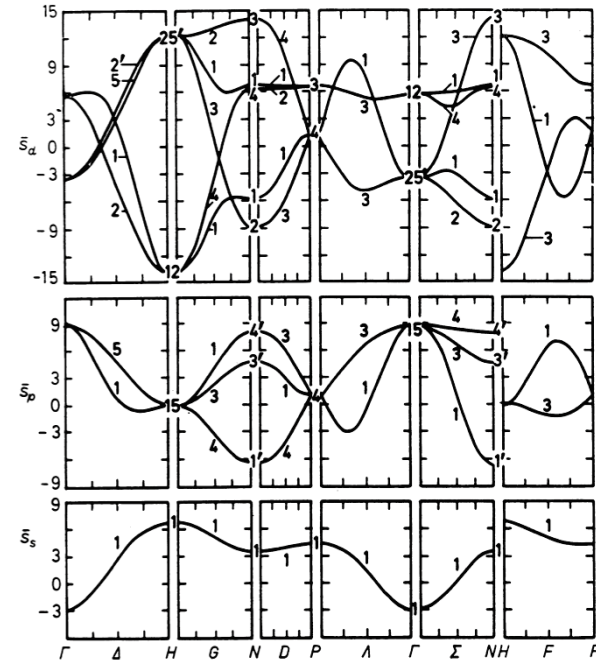
Now, there is only *one* matrix, $K=S$, and four potential parameters,

$$P, \dot{P} = \langle \phi | \phi \rangle, \ddot{P} = 2! \langle \phi | \dot{\phi} \rangle, \text{ and } \dddot{P} = 3! \langle \dot{\phi} | \dot{\phi} \rangle.$$

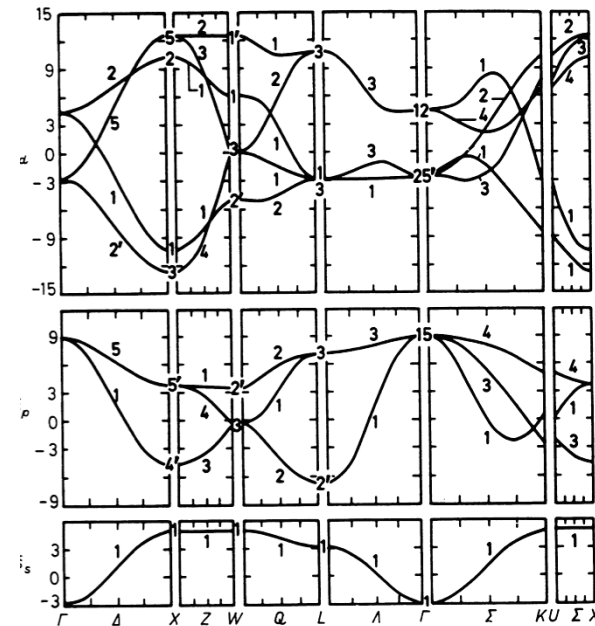
The assumption that the kinked partial waves are orthogonal, therefore constitutes a *generalized atomic-spheres approximation* (ASA) with magic radii q_{Rlm} obtained by the requirement that the potential function satisfies $\dot{P}_{Rlm} = \langle \phi_{Rlm} | \phi_{Rlm} \rangle$. The 1st-order Hamiltonian reduces to:

$$H = \dot{P}^{\frac{1}{2}} E \dot{P}^{-\frac{1}{2}} = \epsilon_\nu - \left(P / \dot{P} \right) + \dot{P}^{-\frac{1}{2}} S \dot{P}^{-\frac{1}{2}}$$

which has the 2-center form, albeit with arbitrary screening.

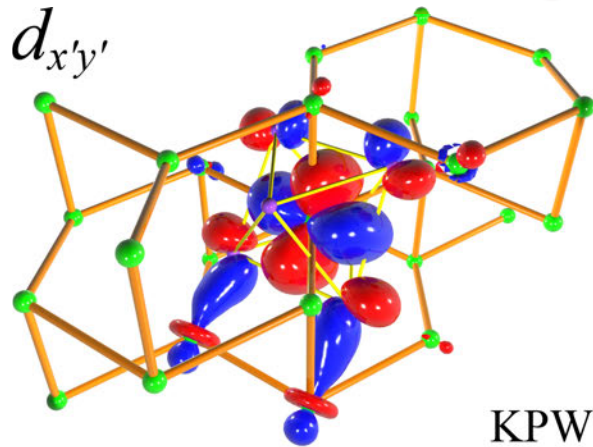


screened canonical s -, p - and d -bands for the b.c.c. structure.

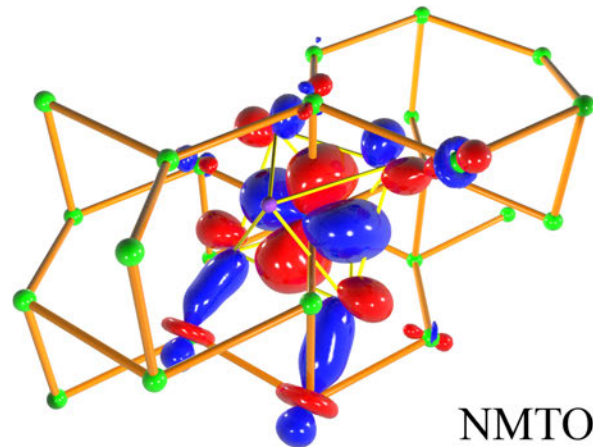


screened canonical s -, p - and d -bands for the f.c.c. structure.

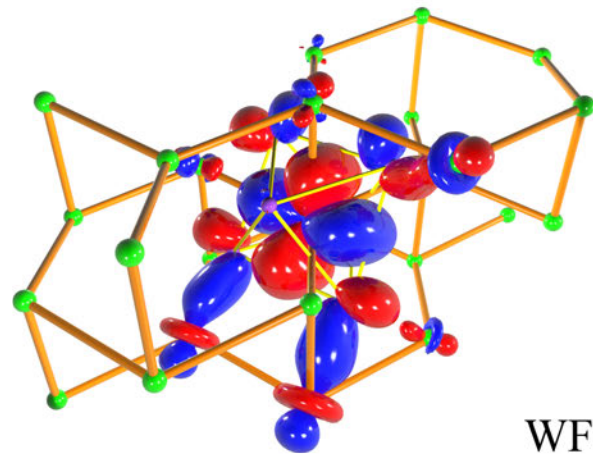
Direct generation of the set of $V t_{2g}$ localized Wannier functions:



The $d_{x'y'}$ member of the $V t_{2g}$ kinked-partial-wave set is a solution of the LDA Schrödinger equation at a chosen energy and has $V t_{2g}$ character at no other site. The KPWs are obtained by downfolding from the complete set of all partial waves at all sites.



The NMTO $V t_{2g}$ set is that linear combination of the KPW sets at the $N+1$ energies chosen, with the property that the NMTO set is complete at those energies. This is N th-order polynomial interpolation for a Hilbert space. The NMTO set has the same size as the KPW set, i.e. its size is independent of N . Hence, there are 3 NMTOs per V site in the $V t_{2g}$ set.

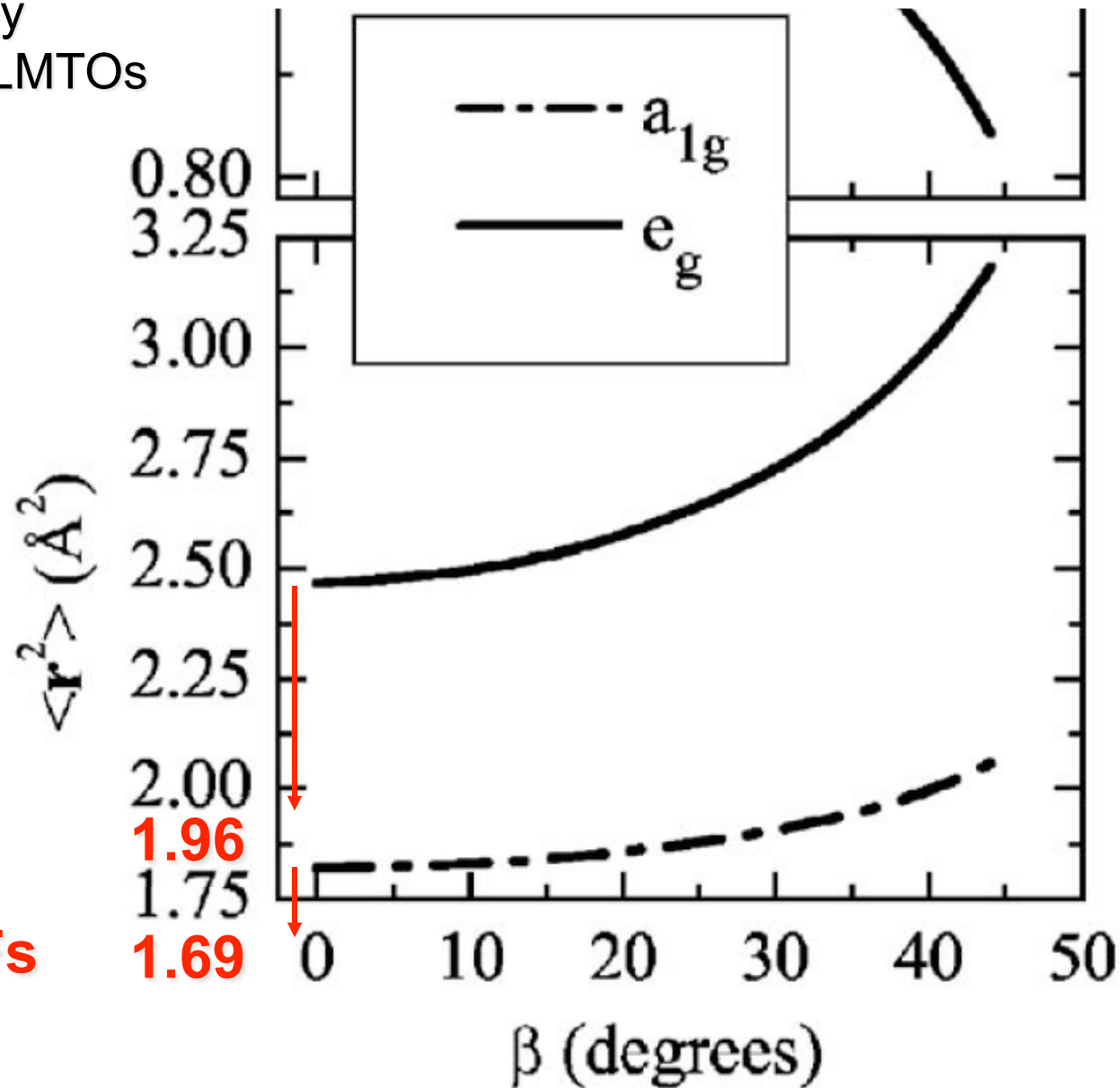


Symmetrical orthonormalization of the (converged) NMTO $V t_{2g}$ set yields a set of localized Wannier functions (WFs).

Taking the spread of the Wannier function as a measure of its localization:

SOLOVYEV, PCHELKINA, AND ANISIMOV PHYSICAL REVIEW B **75**, 045110 (2007)

obtain WFs by
downfolding LMTOs



We:

1.96

NMTO WFs

1.69

5 Standard Löwdin downfolding and N-ization

In the *NMTO* method we first construct the set of energy-dependent, downfolded KPWs (EMTOs) from multiple scattering theory, i.e. we compute the structure matrix in a strongly screened (e.g. *spd*) representation and then downfold this matrix to the desired degree for each energy. *Thereafter* we *N*-ize the EMTOs to form the energy-independent *NMTO* basis set. This is different from standard Löwdin downfolding which partitions a given, large set of energy-independent, strongly localized orbitals into active and passive subsets, $|\chi\rangle = |\chi_A\rangle + |\chi_B\rangle$, and then eliminates the latter. Had one chosen this large basis set to be one of strongly screened *NMTO*s, *N*-ization would have come *before* downfolding, and this is also the sequence in which *LMTTO* downfolding was done in the eighties. Below, we shall first review Löwdin downfolding because it is similar to, but much more familiar than screened multiple scattering theory, and then indicate that *subsequent* use of the *N*-ization technique might be useful.

Partitioning the generalized eigenvalue equations yields:

$$\begin{aligned} (H - \varepsilon O)_{AA} b_A + (H - \varepsilon O)_{AP} b_P &= 0 \\ (H - \varepsilon O)_{PA} b_A + (H - \varepsilon O)_{PP} b_P &= 0 \end{aligned}$$

in block notation. Solving the bottom equations for b_P ,

$$b_P = - [(H - \varepsilon O)_{PP}]^{-1} (H - \varepsilon O)_{PA} b_A, \quad (12)$$

and inserting in the upper equations, yields the well-known set of Löwdin-downfolded secular equations:

$$\left\{ \begin{array}{c} (H - \varepsilon O)_{AA} - \\ (H - \varepsilon O)_{AP} [(H - \varepsilon O)_{PP}]^{-1} (H - \varepsilon O)_{PA} \end{array} \right\} b_A = 0 \quad (13)$$

These, together with the "upfolding" (12) give the exact eigenfunction coefficients $b_I = (b_A, b_P)$, as long as the proper energy dependences are kept. But in order for the secular matrix to have the desirable $H - \varepsilon O$ form, the energy dependence of the complicated matrix $(H - \varepsilon O)_{AP} [(H - \varepsilon O)_{PP}]^{-1} (H - \varepsilon O)_{PA}$ is either neglected or linearized.

We are interested in the set of downfolded *orbitals* giving rise to this secular matrix. This is the energy-dependent set:

$$\begin{aligned} |\phi_A(\varepsilon)\rangle &\equiv |\chi_A\rangle - |\chi_P\rangle [(H - \varepsilon O)_{PP}]^{-1} (H - \varepsilon O)_{PA} \\ &\equiv |\chi_A\rangle + |\chi_P\rangle D_{PA}(\varepsilon), \end{aligned} \quad (14)$$

with each member $|\phi_a(\varepsilon)\rangle$ being the active orbital $|\chi_a\rangle$, *dressed* by an *energy-dependent* linear combination of passive orbitals. How well localized $|\phi_a(\varepsilon)\rangle$ is, depends on how well the chosen set $|\chi_A\rangle$ reproduces the eigenstates at ε .

That the $\mathcal{H} - \varepsilon$ represented in this set is the matrix in (13), is seen by first operating on (14) with $\mathcal{H} - \varepsilon$, and then projecting onto the active and passive subsets:

$$\begin{aligned} \langle \chi_A | \mathcal{H} - \varepsilon | \phi_A(\varepsilon) \rangle &= (H - \varepsilon O)_{AA} \\ &\quad - (H - \varepsilon O)_{AP} [(H - \varepsilon O)_{PP}]^{-1} (H - \varepsilon O)_{PA} \\ \langle \chi_P | \mathcal{H} - \varepsilon | \phi_A(\varepsilon) \rangle &= 0. \end{aligned}$$

Forming finally the linear combination (14) yields the desired result:

$$\begin{aligned} \langle \phi_A(\varepsilon) | \hat{H} - \varepsilon | \phi_A(\varepsilon) \rangle &= (H - \varepsilon O)_{AA} \\ &\quad - (H - \varepsilon O)_{AP} [(H - \varepsilon O)_{PP}]^{-1} (H - \varepsilon O)_{PA} \end{aligned}$$

One can show that this equals $-G_{AA}(\varepsilon)^{-1}$, exactly as in MTO theory. In fact, the entire N -ization procedure developed above could be used to remove the energy dependence of the Löwdin-downfolded set (14).

The result for the dress is:

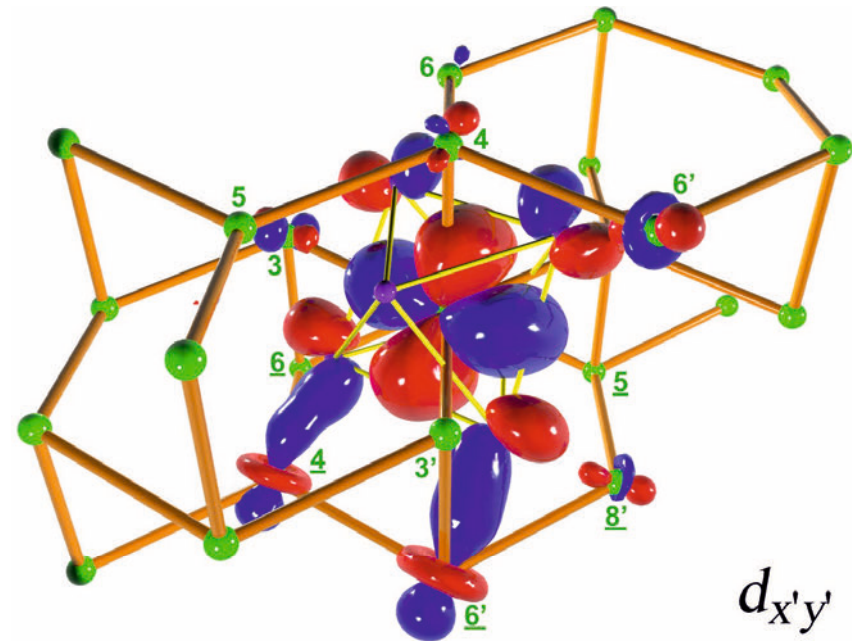
$$\begin{aligned} D_{PA}^{(0..N)} &= G_{PA}[0..N] G_{AA}[0..N]^{-1} \\ &\approx G_{PA}(\varepsilon) G_{AA}(\varepsilon)^{-1} = D_{PA}(\varepsilon), \end{aligned}$$

and therefore the major cause for delocalization seems to be the Löwdin downfolding as given by (14).

This procedure seems to be computationally more demanding than the one we have described, and to yield less localized downfolded orbitals. It certainly only works for orbital basis sets with merely one radial function per Rlm .



$V t_{2g}$ NMTO:

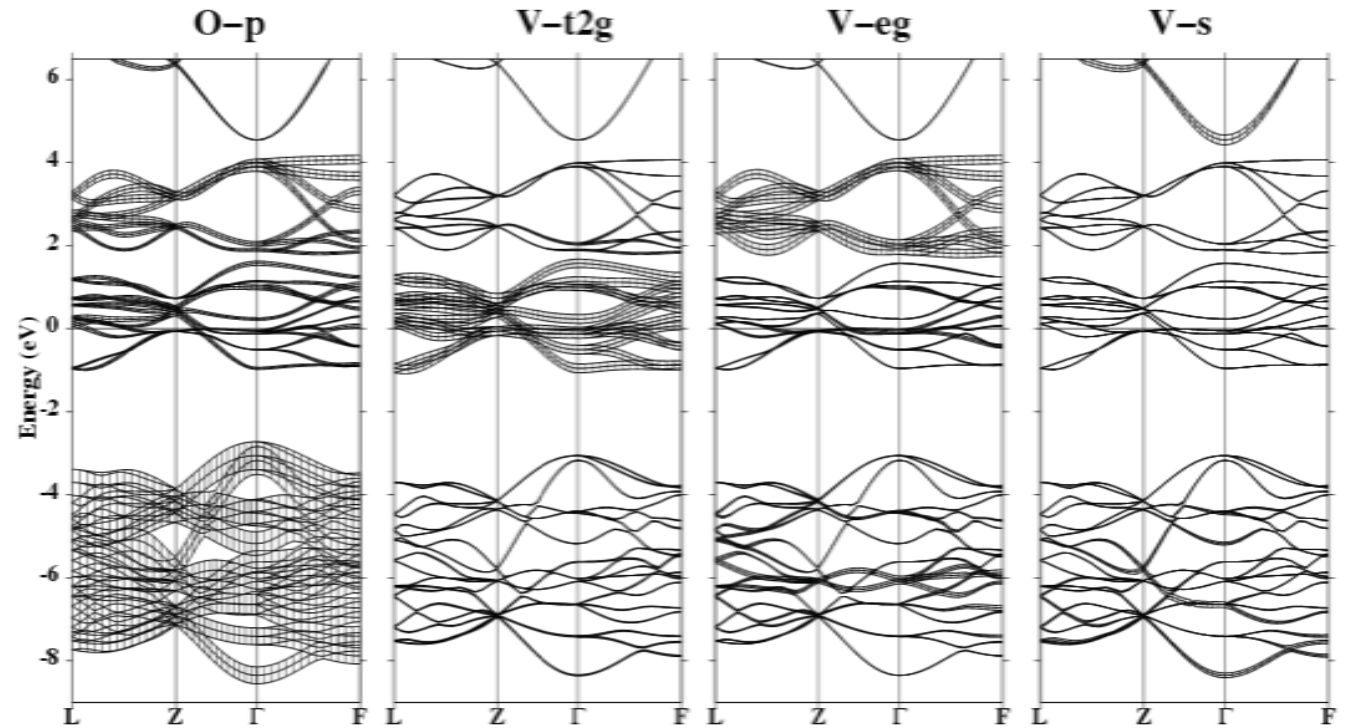


$$|\chi_A^{(N)}\rangle = |\varphi_A\rangle + |\varphi_P\rangle D_{PA}^{(N)}$$



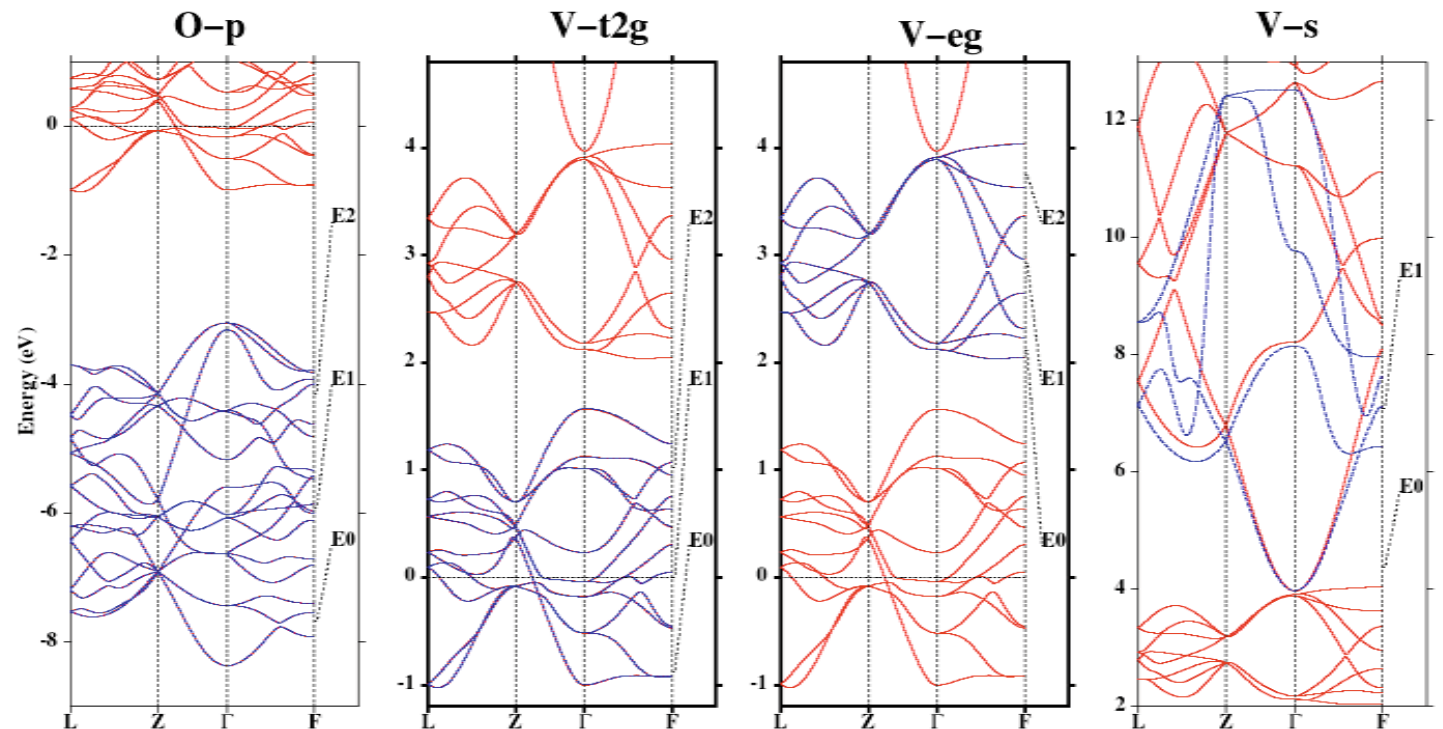
Band structure
obtained with a
large basis set
(LMTO).

Different panels show the
same bands decorated with
various orbital characters
(fat bands)



Band structure,
as above, but obtained
with a large NMTO
basis and shown on
expanded energy scales,
separated into panels.

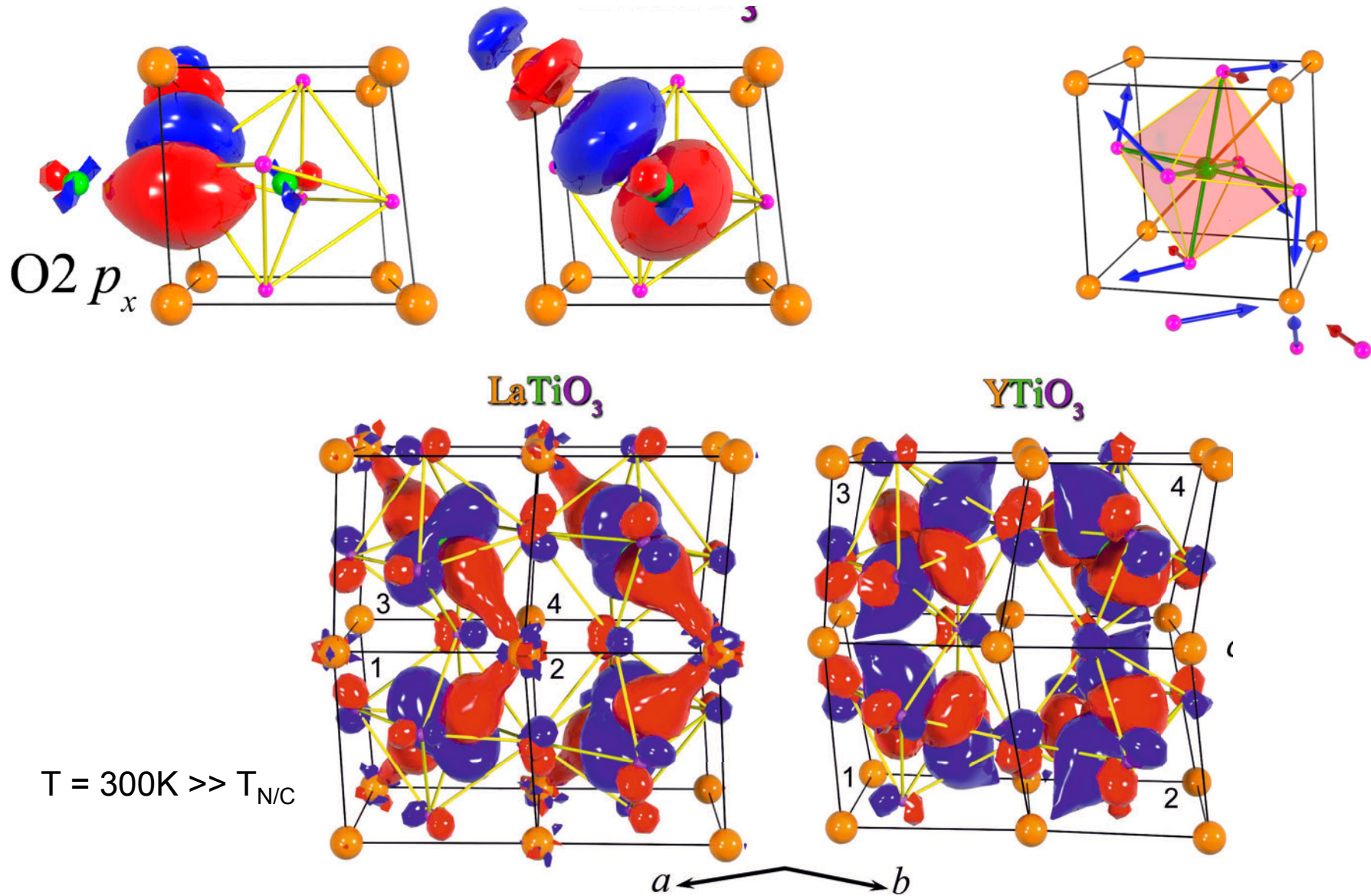
Bands obtained
from Wannier-
functions
(downfolded NMTO)



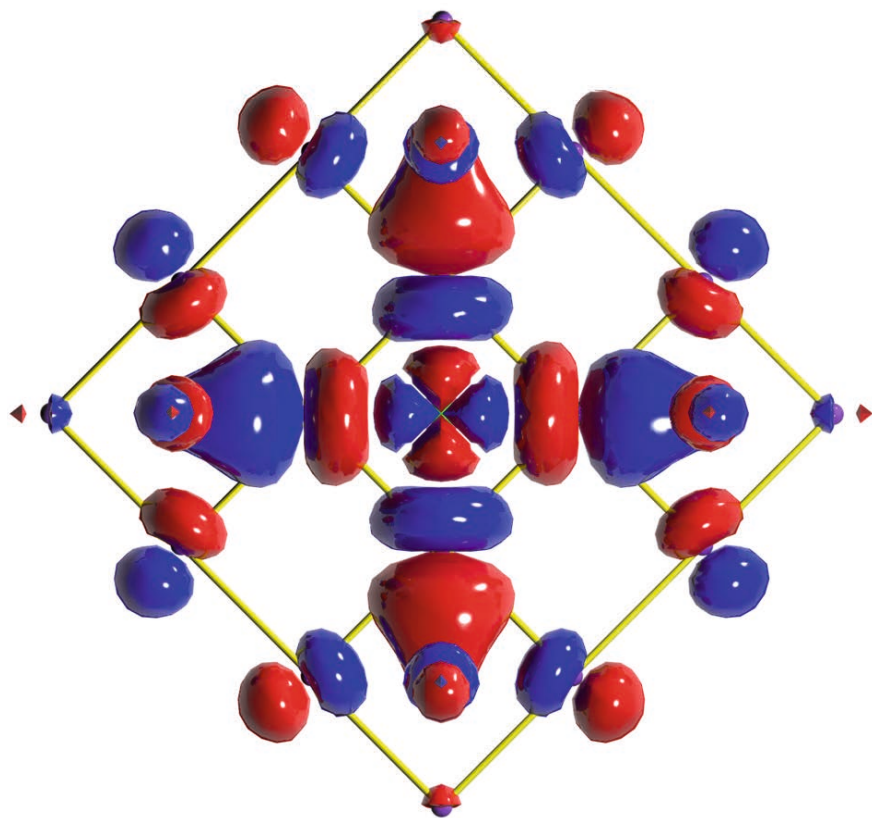
Mott Transition and Suppression of Orbital Fluctuations in Orthorhombic 3d¹ Perovskites

E. Pavarini,¹ S. Biermann,² A. Poteryaev,³ A. I. Lichtenstein,³ A. Georges,² and O. K. Andersen⁴

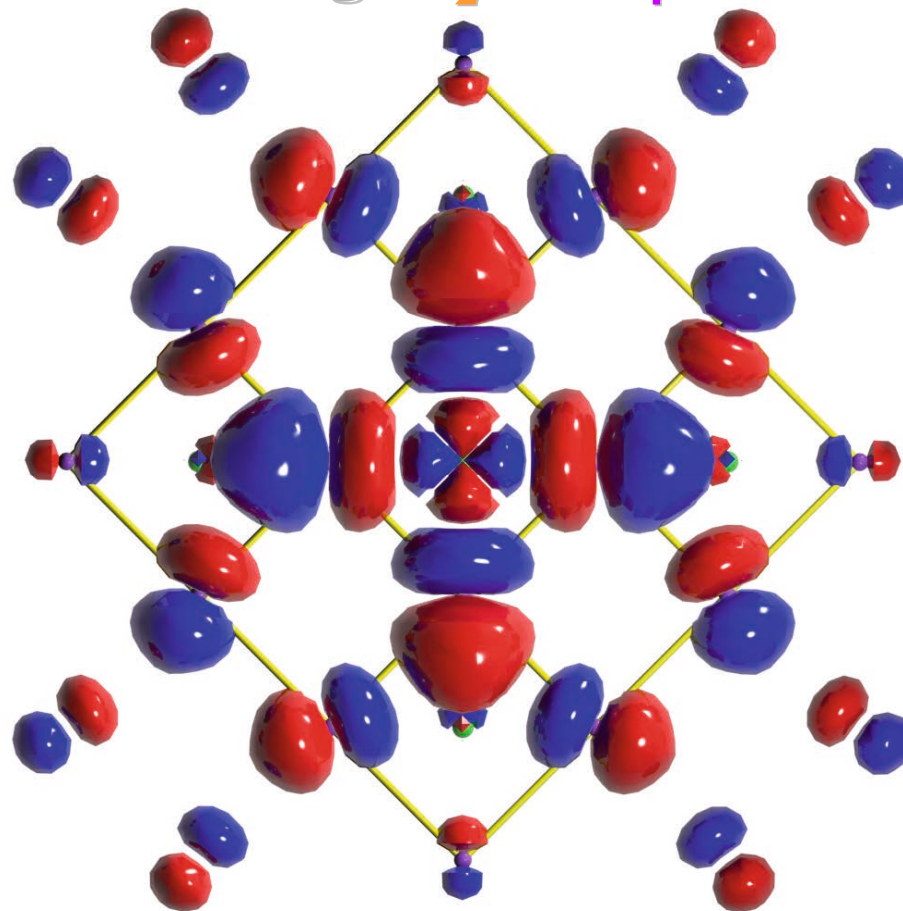
E Pavarini¹, A Yamasaki², J Nuss² and O K Andersen²



One-orbital LDA Wannier-like function

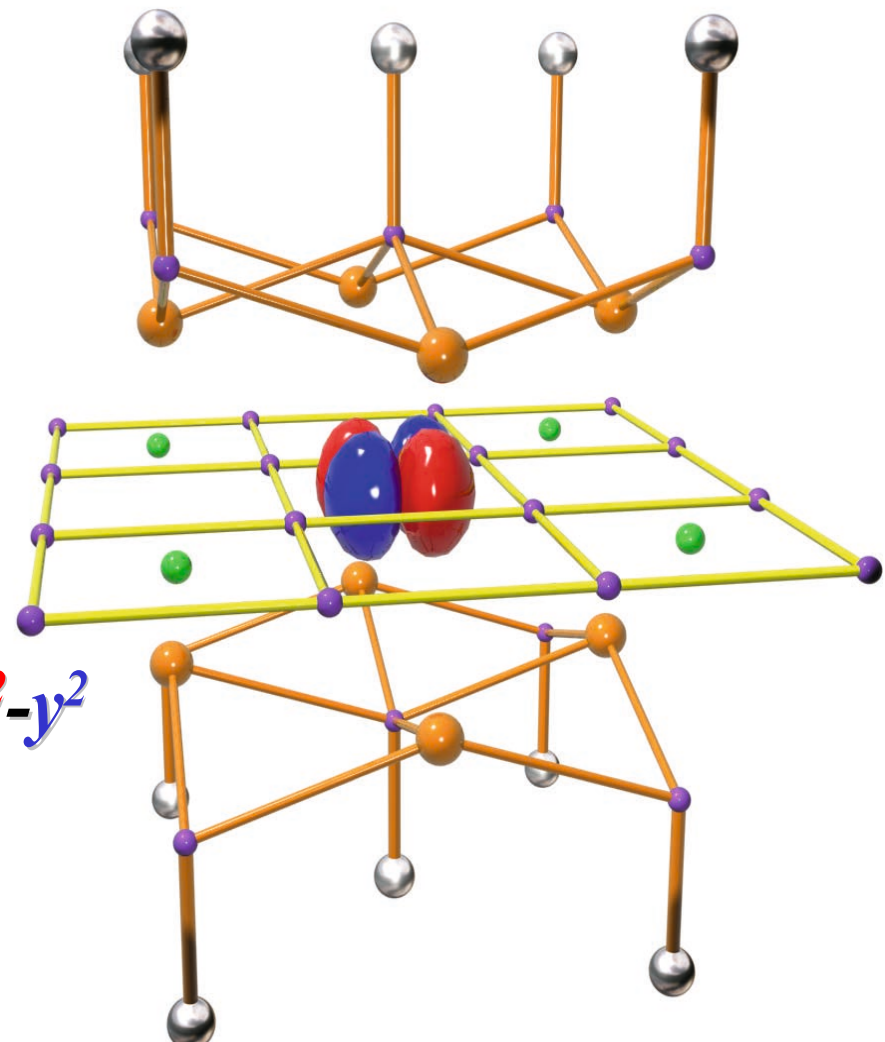
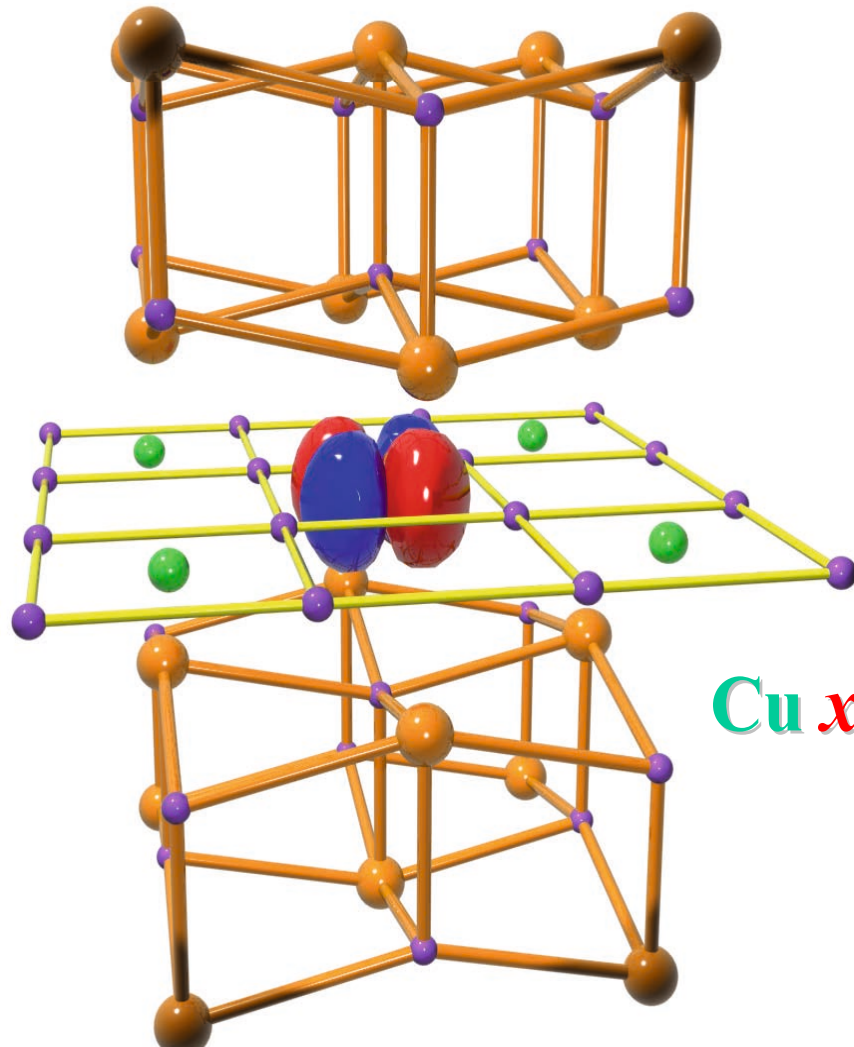


$T_c = 40 \text{ K}, r=0.17$

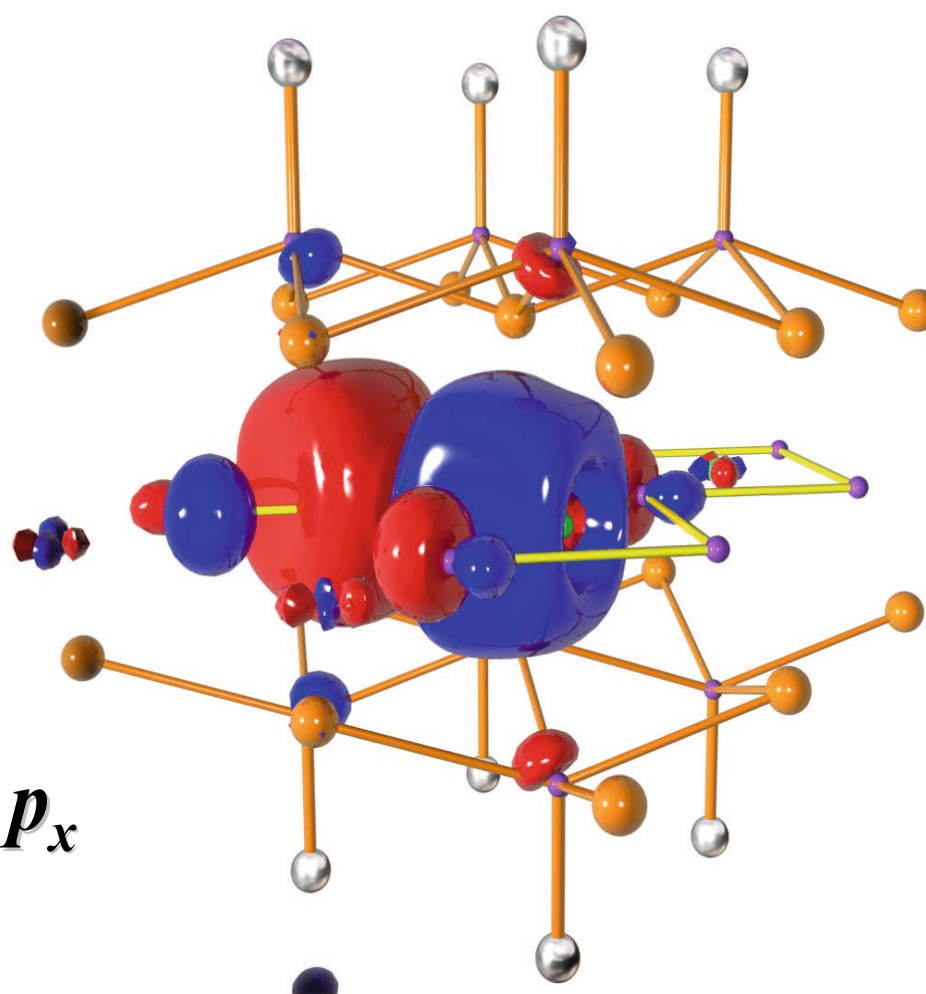
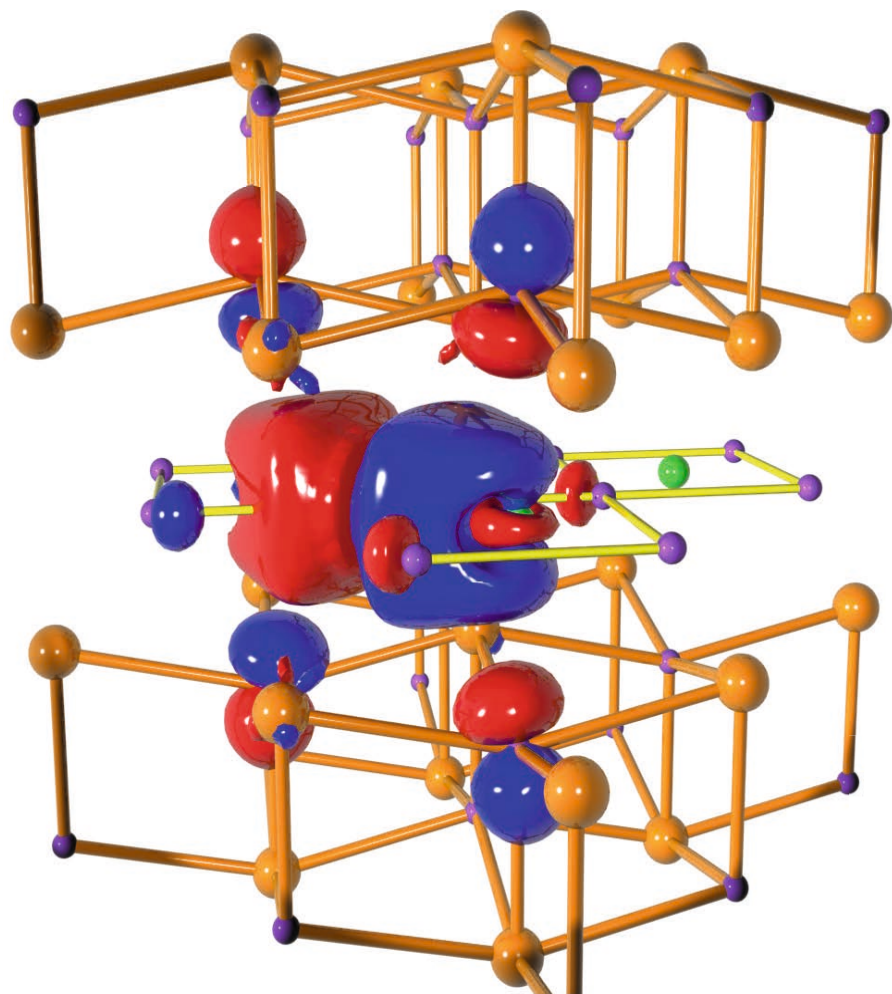


$T_c = 90 \text{ K}, r=0.33$

Three-orbital LDA Wannier-like function



Three-orbital LDA Wannier-like function



$\text{O } p_x$